Development and Application of Covariate Based Reliability Models: Utilizing Constrained Maximum Likelihood Optimization

By

Robert Kosaka

A thesis submitted to the

Graduate School-New Brunswick

Rutgers, The State University of New Jersey

in partial fulfillment of the requirements

for the degree of

Masters of Science

Graduate Program in Industrial and Systems Engineering

Written under the direction of

Dr. David Coit

and approved by

New Brunswick, New Jersey

May, 2013

ABSTRACT OF THE THESIS

Development and Application of Covariate Based Reliability Models: Utilizing Constrained Maximum Likelihood Optimization

By Robert Kosaka

Thesis Director:

Dr. David Coit

In this research, a difficult yet practical problem of modeling failures as functions of stress profiles was addressed. Failures, both system and component based, can in many cases be explained in terms of the stresses experienced. These stresses are crucial in understanding the reliability of the component or system. If the underlying stresses can be determined, it becomes possible to create reliability models that incorporate them. In many cases reliability models can be made independent of stresses or in terms of a single stress. In this scenario the process of building the respective reliability model is not complex. These simple scenarios that have a limited number of stresses do not necessarily demand a rigid algorithm. When creating a reliability model for a single, or perhaps a system that experiences two stresses, trial-and-error is sufficient. Problems arise however when a system undergoes an excessive number of different stresses. These stresses all impact the system differently, and thus they must be modeled accordingly. Such a trial-and-error method would not be practical or appropriate. The primary goal of this research is to develop algorithms that can systemically approach these situations. In the case of the research, the system under study experiences a variable load profile. This

algorithm aims to create an approach that can accurately capture the system reliability, while factoring in the system stresses.

US Navy NAVAIR, in recent time, has had an increased interest in studying system and component reliability. This is in part due to the large amount of resources that corrective actions and preventative maintenance require. These failures however, are based on the current system stress profile. Currently, the Navy has plans for a changing stress profile, as there will be a change in air wing composition. This changing stress profile is predicted to negatively impact system reliability. It is possible however, to create predictive models using the current and past failure data. This modeling approach utilizes a two parameter Weibull distribution to account for a changing stress profile. Inputs into this model are the anticipated composition of the naval air wing.

Acknowledgements

The completion of this thesis could not have been possible without the faculty of Rutgers, as well as the staff a NAVAIR's Lakehurst facility. I could not have succeeded in completing this thesis without their support and guidance.

Firstly I would like to express my gratitude to the US Navy and Naval Air Systems Command, for without them this opportunity would have never existed. Their funding of research at Rutgers University has given me the opportunity to pursue a graduate education. Specifically I would like to thank the staff at NAVAIR's Lakehurst facility including Mark Agnello, Dona Johnson, and Keith Megow. Their knowledge of the systems studied in this research made this thesis possible.

I would like to especially thank my advisor Dr. David Coit, whose expertise and vast experience in the field of reliability engineering proved invaluable. It goes without saying that he made the completion of this thesis possible. Dr. Coit introduced me to the world of reliability engineering, something I will always be grateful for. Watching him work gave me the inspiration necessary to complete the graduate curriculum, and showed me what could be done with said education.

I would also like to thank the members of my thesis committee, Dr. Melike Baykal-Gursoy and Dr. James Luxhoj, who provided me with feedback and motivation. Their words of advice will not be forgotten and it has been an experience I will always remember.

Dedication

To my grandparents Fusaye and Masato Kosaka.

Table of Contents

List of Figures

List of Tables

Table 1: Table of Definitions

BT	Bridle Tensioner
IPA	Improved Piston Assembly
NGL	Nose Gear Launcher
WB	Water Brake
NAVAIR	Naval Air Systems Command
Air Wing	Types of aircraft in use

1.0 Introduction

Analyzing reliability data is a multi-step process that can give insight related to design decisions, as well as creating maintenance policies. Failures of a component, in most cases, can be traced to environmental conditions, material properties, or stresses. The importance of this is that it allows for the determination of causation for the respective failure. This correlation of stress or environmental condition allows for the usage of reliability modeling.

This research thesis is intended to evaluate the different modeling approaches applied to data obtained from loading systems with quantifiable loading patterns. Every use of this system is unique with respect to the stresses seen by the system. This data makes it possible to then create stress and failure distributions to describe past events. In the case of the system under study, the stress profile is anticipated to undergo a shift in the near future.

Given that there is a changing stress profile, it is important from the user's perspective to understand the possible impact. The primary focus of this research is to create an approach to develop predictive models using such data. Given the past failure data, and the known shift, it is possible to create such models. This research aims at developing multiple approaches to address this situation by creating predictive, stress-based reliability models.

1.2 Background

A primary source of sponsorship and information is NAVAIR, or Naval Air Systems Command. This division of the government provides system support and technological development for the US Navy. The division that has been working directly with this research is located in Lakehurst NJ. This division specializes in support equipment for launcher and recovery gear for aircraft carriers. Together, these systems allow for the usage of aircraft on carriers.

The recovery gear, also known as arresting gear, is the system that is responsible for allowing aircraft to land on aircraft carriers. The primary components of this system include pendants, purchase cables, sheaves, and the arresting engine. Purchase cables are cables strung across the deck of the ship and are what the aircraft attach to when landing. The arresting engine absorbs shock of the aircraft attaching to the purchasing cables. Sheaves direct the purchasing cable and ensure that it has an unobstructed path. Pendants are the components that attach to the plane itself, and are located on the purchasing cable.

The launcher, or catapult, is the system responsible for accelerating the aircraft to take-off speed. Due to the limited runway distance, additional acceleration from the catapult is necessary. The system itself consists of two large cylinders, each of which contains a piston. These pistons are forced down their respective tube by means of steam pressure. After take-off the pistons are decelerated by a component known as the water brake. This component uses water pressure to resist the force of the incoming piston.

Air wing composition is critical in the performance of a carrier's operations. The air wing is comprised of different types of aircraft, each of which performs a unique role. Aircraft currently in use include; F/A-18E/F, F/A-18C, EA-6B, E-2C, C-2, and T-45. Each of these aircraft when launched or arrested, has a unique stress profile, because of this, each aircraft impacts system degradation differently.

1.3 Problem Statement

Over the course of time, the US Navy has phased out older aircraft and replaced them with more advanced successors. These newer aircraft are not only more complex, but they are also much heavier than their predecessors. This is due to both design, as well as the payload of electronics and weapons. Newer aircraft generally carry more weapons, as well as more fuel due to a changing mission profile. This trend is expected to increase over the next twenty years. A major concern is possible impact this trend may have on component reliability. There exists much concern within the Navy that this increasing trend will have a negative impact on component reliability. Because of this, predictions of component reliability must be made for the future state to verify these concerns.

1.4 Study Objective

The initial objective of this research is to develop reliability models as a function of system stresses. This is possible due to the available failure data of the system's components. Each failure in the system can be described by system stresses. The analysis of stresses, and the importance of their impact, is being determined with the aid of in-service engineers. These models are based on the two-parameter Weibull distribution, with the scale parameter being a mathematical function of the respective stresses. In doing this, it becomes possible to make future predictions of system reliability.

Such predictions also aid in creating optimal preventative maintenance policies to reduce unexpected corrective actions. The current maintenance and replacement policies are designed for historic air wings. That is to say that the composition or aircraft that they were designed to accommodate are no longer in use. In-service engineers anticipate that these maintenance and replacement policies are not applicable to the current and predicted usage of the carrier systems. Because of this, updated policies must be created based on current and predicted system usage. These policies can be estimated from the created reliability predictions.

2.0 Literature Review

A study of published research studies was conducted to understand current modeling techniques and replacement policies. These research works include-stress based reliability modeling, optimal replacement, accelerated life testing, as well as their respective applications. These research studies provide insight into the underlying methods of this research.

2.1 Data Mining and Component Replacement

Component replacement is essential to maintain an operating system. This can however, be expensive and time consuming. Because of this it can be beneficial to determine or predict when replacements are necessary. Work done by Letourneau et al (1991) sought to create predictive models from aircraft sensor data. Their work used flight and performance data from aircraft to develop models. These models were not all inclusive however, and could only be done for specific aircraft components. Figure 1 shows the process from the data collection to the final model.

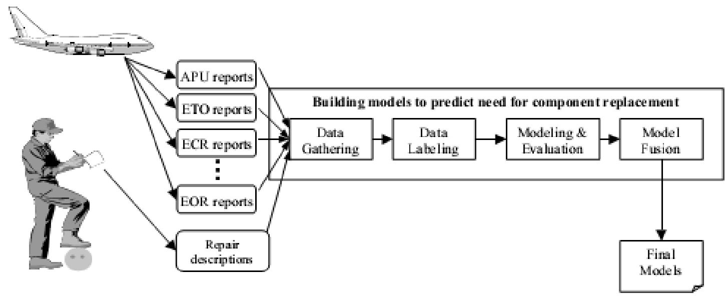

Figure 1: Information Flow Diagram (Letourneau et al, 1991)

Letourneau et al (1991) state that sensor data must be filtered and properly selected to correctly utilize their approach. This is necessary due to the random false readings of the sensors. They state that random sampling is not appropriate, as it is essential to select data near a replacement interval. Replacement data is mined from a database that contains all maintenance activity. This database includes information regarding the component, time of replacement, and a textual description of the actions taken. Figure 2 is a visual representation of how the data is accessed while in the databases. It can be seen that there exist different datasets, each with a unique set of properties.

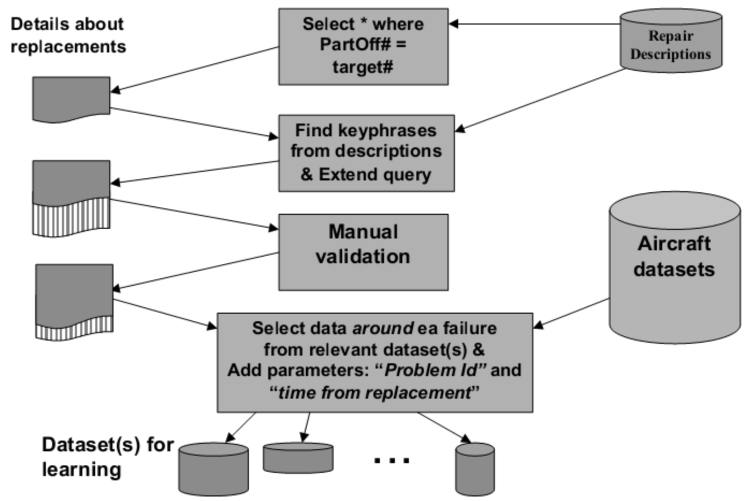

Figure 2: Data Storage and Access (Letourneau et al, 1991)

The data that was collected was then used to create reliability models. To infer these models, techniques such as decision trees, rough sets, regression, and neural networks could be used. Letourneau et al (1991) also state that depending on the technique used, additional preprocessing could be required. This additional preprocessing includes normalizing the attributes, creating new attributes, selection of the most suitable attributes, or usage of discrete continuous attributes.

The components under study could be replaced for one of two reasons, the first being regular maintenance. This regular maintenance is imposed by aerospace regulations, or the airline's policy. In this case the component has not technically failed and is being prematurely removed from the system. The second type of replacement is when the component has reached a deteriorated state and must be replaced. Letourneau et al (1991) state that this second type of replacement requires predictive models.

Furthermore they state that these models can only be created when there exists sufficient failure data.

Letourneau et al (1991) explain that this approach is not all inclusive, and does not detect all possible failure modes. Failures due to poor maintenance, as well as due to design flaws, cannot accurately be detected with this approach. This is in part due to a lack of data concerning maintenance actions and design of components. They state that this does not raise concerns, as failures due to these modes are not common.

A reward function was developed which generated a reward for predicting the correct outcome. In the most basic form the reward threshold were fixed values between 0 and 1. In application, they varied the reward threshold for different instances. Each component had a distinct function that computed the reward of predicting a correct result. For this case, a correct result was a replacement time at a specific time less than the expect failure, referred to as the target interval. Figure 3 shows a graph of the reward function. It can be seen that the reward is generated when the replacement it performed within a specific interval before the failure.

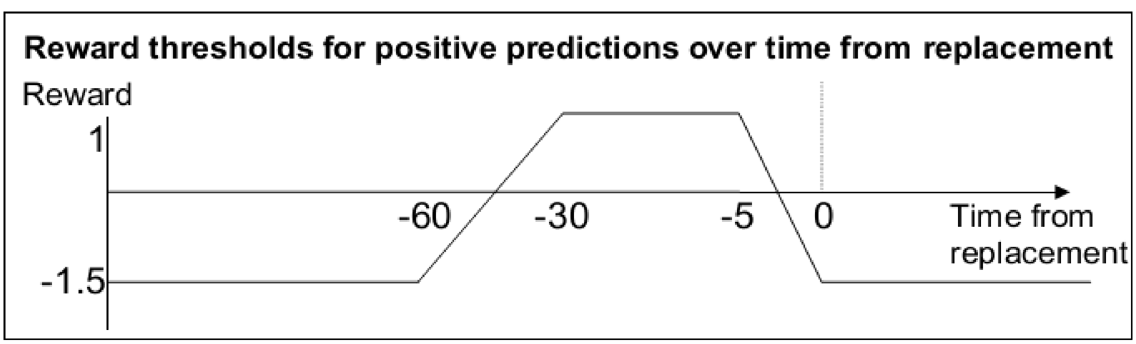

Figure 3: Reward Threshold (Letourneau et al, 1991)

A scoring metric was developed to determine the performance of the model. This evaluates the coverage of a model by looking at the distribution of alerts over the failure cases. This scoring metric can be seen in Equation 1. The term $score_i$ is the score form the reward function for the i^{th} instance classified. *NbrDectected* is the number of replacement cases that have at least one positive prediction in the target interval. *NbrOfCases* is the total number of replacements for a given component. The term *SignSumOfScores* is the sign of the first term in the expression.

$$score = \left(\sum_{i=1}^{p} score_i \right) \left(NbrDetected / NrbOfCases \right)^{SignOfSumOfScores} \qquad (1)$$

2.3 Age Replacement of Components

Work done by Das and Acharya (2004) proposed two alternative policies for preventative replacement of a component with degrading performance. The components under study show signs of occurrence of a fault, and operate for a given time with degraded performance, before failure. Time between fault occurrences is termed as delay time. The two policies for replacement are age replacement during delay time policy (ARDT), and opportunistic age replacement during delay time policy (OARDT). Each policy has distinct advantages and disadvantages.

Replacement policies are intended to ensure maximum utilization of component life. While age replacement has advantages over block replacement and group replacement, it requires continuous tracking of component service life. This can be a difficult task, especially if there are there numerous systems that are comprised of multiple components. Options to overcome this, including on-line instruments, are often expensive to purchase and implement.

In many cases components have indicators before a failure. These include increases in temperature, vibration level, increased defects in final products, as well as other indicators. These are referred to by Das and Acharya (2004) as fault indicators in their study. Fault indicators, in many instances, do not require the usage of complex and costly monitoring devices. These attributes are often captured during routine system or component maintenance. They state that these indicators do not imply an immediate failure, but a degradation of the component. There exists a lag time between the discovery of the fault indicator and the final failure of the component.

Age replacement during delay time policy requires the usage of these fault indicators. In this policy, replacement is done following the detection of a fault indicator. The goal is to minimize the long run cost per unit time by finding the optimal replacement time. The long run cost per unit time is given by Equation 2.

$$G_d\left(t_d\right) = \frac{\text{expected cost during life cycle}}{\text{expected length of life cycle}} = \frac{C_d(t_d)}{L_d(t_d)} \tag{2}$$

where:

$G_d(t_d) =$ Long run cost per unit

Das and Acharya state that the expected cost in a renewal cycle is the sum of expected preventative replacement cost, the expected failure replacement cost, and the expected cumulative degradation cost per renewal cycle. To express this Equation 3 is used. C_r is expressed as the expected cumulative degradation cost over a renewal cycle.

$$C_d(t_d) = C_p[1 - F_H(t_d)] + C_f F_H(t_d) + \{C_r(\min(H, t_d))\} \tag{3}$$

A similar set of equations was developed for OARDT, which can be seen in Equations 4 and 5. In the case of OARDT, the cost of a renewal cycle is the sum of the expected cumulative degradation costs and the expected replacement cost.

$$G_{od}(t_d) = \frac{\text{expected cost during life cycle with opportunistic replacement}}{\text{expected legnth of life cycle with opportunistic replacement}} = \frac{C_{od}(t_d)}{L_{od}(t_d)} \tag{4}$$

$$C_{od}(t_d) = C_r(\min(H, t_d + Y)) + C_0[1 - F_H(t_d + Y)] + C_f F_H(t_d + Y) \tag{5}$$

2.4 Modeling Failure Rate with Respect to the Number of Load Applications

Research done by Wang et al (2007) sought to model the failure rate of components as a function of load applications. This was done by taking static strength failure and fatigue failure as the backgrounds, and in turn, the dynamic reliability models with and without degradation could then be derived. The failure rate of each component modeled, with respect to the number of load applications, is made possible by these reliability models. They found that it was possible to model these failure rates for systems with and without degradation. From their work they found that without degradation, both reliability and the failure rate decrease with respect to the number of loads applied.

The first step in their approach was to develop reliability model for a component under repeated random load. They sought to create reliability models, where life is measured by the number of load applications. There were two scenarios for this approach, with and without degradation of strength. Wang et al (2007) state when strength is not impacted by loads, the loading profile can be simplified. This special case occurs when a component undergoes n random loads and does not fail under the maximum load. From this it can be concluded that the reliability when load is applied n times equal the maximum load of the n load samples applied a single time. When this concept was applied to a reliability model, Equation 6 was developed. In this $f_\delta(\delta)$ represents the pdf of a random variable with original strength δ.

$$\begin{aligned} R(n) &= \int_0^{+\infty} f_\delta(\delta) \int_0^{\delta} n\left[F_s(x)\right]^{n-1} f_s(x)dx\, d\delta \\ R(n) &= \int_0^{+\infty} f_{\delta}(\delta)\left[F_s(\delta)\right]^n d\delta \end{aligned} \tag{6}$$

In the case of degenerative strength, each load decreases the strength of a component a certain amount. In practice the degree of degradation is relative to the magnitude of the load. When the magnitude of the loads experienced is constant, the residual strength of the component can be modeled as a function of the magnitude of the load and the number of load applications.

Wang et al (2007) modeled the residual strength when the variance of the magnitude of loads was constant. μ_s is the mean load and is a constant value, N_{μ_s} is the fatigue life corresponding to the load level s, and c is the material coefficient. From this Equation 7 can be formed.

$$\delta_n = \delta - (\delta - \mu_s)\left(\frac{n}{N_{\mu_s}}\right)^c \tag{7}$$

From the residual life model it can be determined whether the n^{th} load cycle causes a failure of the component. This can be seen in Equation 8, which extends

Equation 7. In this model A_n represents the event that a component does not fail after the n^{th} load.

$$P\left(A_n \mid \delta\right) = \int_0^{\delta_{(n-1)}} f_s(s)ds = F_s\left(\delta_{(n-1)}\right) \tag{8}$$

Using Equations 7 and 8 it is possible to develop a reliability model that incorporates both strength and stress. Wang et al (2007) created a reliability model that considers both the original strength δ, which is a random variable with pdf $f_\delta(\delta)$. The reliability for a component, when random load is applied n times is defined by Equation 9.

$$\begin{aligned} R(n) &= \int_0^{+\infty} f_\delta(\delta) \prod_{i=1}^{n} \int_0^{\delta_{(i-1)}} f_s(s)dsd\delta \\ R(n) &= \int_0^{+\infty} f_{\delta}(\delta) \prod_{i=1}^{n} F_s(\delta, i-1)d\delta \end{aligned} \tag{9}$$

The failure rate for a component without degradation, when plotted against number of load cycles, had a partial bathtub curve and can be seen in Figure 4. In the case of the system with degradation, the reliability of the component had a much more pronounced decrease which is located in Figure 5. Likewise it was found that the failure rate curve was a bathtub shape. This outcome is to be expected, as the effects of degradation should have an undesirable impact on the failure rate, i.e., higher failure rate.

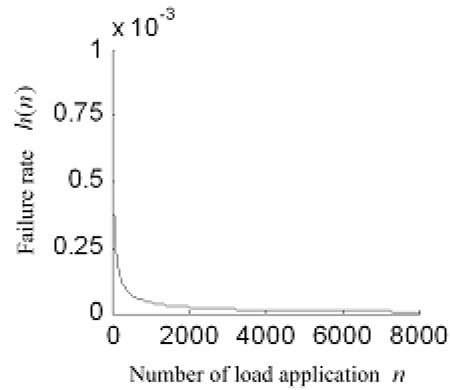

Figure 4: No Degradation pdf (Wang et al, 2007)

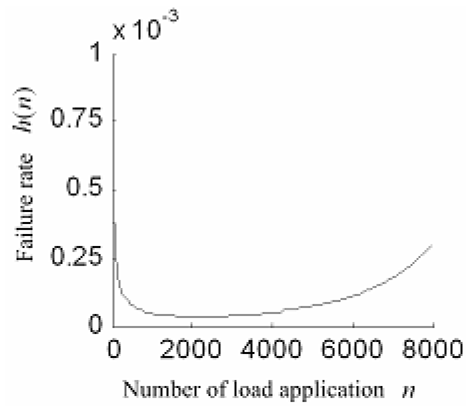

Figure 5: Degradation pdf (Wand et al, 2007)

2.4 Reliability Models Considering Operating Conditions

Research conducted by Prasad (2002) modeled proportional hazard rates to investigate the effects of diagnostic variables on a system's life. He states that in many cases failure time is only considered when modeling reliability. He states that it is important to consider factors such as the type of failure and the various stresses in the reliability function. When factored into the reliability model, these are known as covariates and the model is known as a proportional hazard model. In his work two types of data were studied; renewal process data and non-renewal process data. Different approaches to estimation of cumulative hazard rate function include parametric and non-parametric models. In his research goodness-of-fit was used to verify the assumption of the proportional hazard model. Parametric models including the Weibull distribution or Power Law process are fitted to check results obtained using non-parametric models. In his work, Prasad (2002) uses failure data of electro-mechanical equipment utilized in a mine. One of the goals in his research was the development of optimal preventative maintenance intervals for the equipment under study.

The hazard rate of equipment, in proportional hazard modeling, is a function of time and system covariates. It is the product of an unspecified baseline hazard rate $\lambda_0(t)$ and an exponential function comprised of covariates. This can be seen in Equation 10. In this equation z is a vector consisting of covariates. The term β is a vector of regression coefficients. The baseline hazard function is not fitted into a specific model and is of non-parametric form. It represents the hazard function when all covariates take on a value of zero.

$$\lambda(t,z) = \lambda_0(t) \times \exp(z\beta) \tag{10}$$

In order to estimate the regression coefficients the partial likelihood function must be maximized. The partial likelihood is the product over all failure times of the conditional probability of failure of the item, which failed at time t_i. For the proportional hazard models, the partial likelihood function can be seen in Equation 11. d_i is the number of tied failure times, which is small when compared to the number of items j in the risk set at time t_i. Once estimated, the values of β are tested for significance. This ensures that each covariate has an effect on the behavior of the system. From this the reliability equation can be created, as seen in Equation 12. This reliability equation is a function of both time and covariates.

$$L = \prod_{i} \left\{ \exp(z_i \beta) \middle/ \left[\sum_{j \in NF_i} \exp(z_j \beta) \right]^{d_i} \right\}$$
$$\text{where:} \tag{11}$$
$$L = \text{Partial Likelihood}$$

$$R(t,z) = R_0(t)^{\exp(z\beta)} \tag{12}$$

Prasad (2002) explains that the parametric modeling approach is vital in situations where extrapolation of results is necessary to predict failure rates under different conditions than those under study. He states that if failure data is reasonably modeled by a parametric distribution, the parametric approach will provide better information when assessing properties of the baseline hazard function. The Weibull distribution, according to Prasad, is known to fit many failure processes well. Equation 13 shows this reliability function as a function of covariates. In this function z_i are explanatory variables, or covariates, where z_0=1. The values of a_i and the shape parameter δ are unknown and must be estimated. The hazard function is denoted by Equation 14.

$$R(t) = \exp\left\{ -\left[t \middle/ \exp\left(\sum_{i=0}^{k} a_i z_i \right) \right]^{\delta} \right\} \tag{13}$$

$$\lambda(t,z) = \delta \times t^{\delta-1} \big/ \left[\alpha(z) \right]^{\delta} \tag{14}$$

In block replacement maintenance activities are carried out at regular intervals of time. This is done regardless of previous planned maintenance actions. It is assumed that planned maintenance action brings the system to a renewed condition. An unplanned maintenance action, however, retains the system in the bad-as-old condition. If *c* is the average cost of planned maintenance, and *d* is the average cost of maintenance, the average cost per unit time is defined by Equation 15. $E(N(t),z)$ is the expected number of failures in the time interval $(0,t]$ and c/d is the cost ratio.

$$C(t) = \left(c + d \times E\left[N(t), z\right]\right)/t = d\left((c/d) + E\left[N(t), z\right]\right)/t \tag{15}$$

2.6 Mixed Weibull Model

Mixed Weibull models can be used to represent a component that experiences multiple failure modes. This is illustrated in the work done by Attardi et al (2008), who studied the reliability of automotive components. In their work they studied components installed in different car types, which in turn yielded different operating conditions. Because of this, the failure time of each component was considered a random variable with a bimodal probability density function that is also dependent on a vector of covariates that index the operating conditions. This vector of covariates translates back to the Weibull model, where the scale parameter is a function of this vector. Attadari at al (2008) developed an algorithm for maximum likelihood estimation to test the significance of covariates as well as constrict a regression model.

To develop the parametric model a set of assumptions were developed. These assumptions assured that the application of the model was valid and that the results had meaning. From these assumptions, the survival function can be developed as is seen in Equation 16. This model is based on the following assumptions.

- The reference population is a mixture of two subpopulations, each with an unknown mixture.
- Each subpopulation represents a unique failure mode, and an item in a subpopulation can have only one failure mode.
- Items in the reference population experience different operating conditions.
- Due to the fact that car dealerships do not conduct post-mortem analysis, it is impossible to determine what subpopulation an item belongs to after failure.
- The survival function of items is a two-parameter Weibull model based on proportional hazards model. Covariates only act on the scale parameter.

$$R(t \mid x) = \sum_{i=1}^{2} p_i \exp\left[-\left(\frac{t}{\alpha_{i0} \exp(x\delta_i)} \right)^{\beta_i} \right] \tag{16}$$

The set of grouped data is composed of M=3 subsets of grouped data, each representing a different operating condition. This is then indexed by a vector of covariates x_m (m=1,2,3). The likelihood function for used is this research is denoted in Equation 17.

$$
\begin{aligned}
L(\theta,\delta_1,\delta_2) &= \prod_{m=1}^{3} L_m(\theta,\delta_1,\delta_2) \\
&= \prod_{m=1}^{3}\left\{\prod_{i=1}^{N}\left[R(t_{i-1}\mid x_m)-R(t_i\mid x_m)\right]^{f_{i,m}}\left[R((t_{i-1}+t_i)/2\mid x_m\right]^{c_{i,m}}\right\}\bullet\left[R(t_N\mid x_m)\right]^{r_{N+1,m}}
\end{aligned}
\tag{17}
$$

Using these equations, and the approaches outlined in their research, Attardi et al were able to determine the effects of different operating conditions using a mixed Weibull model. Their approach concluded that only one of the factors influenced the model significantly. This ability to model the impact of operating conditions, as well as determine their significance, is quite profound.

2.7 Reliability Modeling With Failure Statistics

Work done by Zhang and Gockenbach (2007) used failure data to develop reliability models for electrical components. In their work they modeled reliability due to electrical stress, mechanical stress, temperature, and time. They state that the proposed models accurately predict reliability and failure rates based on these factors. The models created were not only parameterized with a large amount of statistical data, but also determined by aging tests and breakdown tests available for the probabilistic assessment.

Evaluation of the failure statistic is dependent on both the quality and quantity of the available data. In their work, Zhang and Gockenbach (2007) had failure data from a long range of time periods. Despite this, information on specific damage was difficult or impossible to acquire. A primary goal for their research was to collect robust historical failure data to develop a failure statistic. This detailed failure statistic would provide information about the conditions of the electrical equipment whose failure probability can be modeled.

Accurately modeling the reliability of the component utilized multiple reliability models. These include the Arrhenius model, and the inverse power model. These two models were used to relate the system stresses in terms of reliability of the components. An electro-thermal model was created by combining these two concepts and can be seen in Equation 18.

$$L = L_0 (E/E_0)^{-(n-bt)} (M/M_0)^{-m} e^{-BT}, T = 1/\vartheta_0 - 1/\vartheta(1) \tag{18}$$

This is done assuming that the aging rate under the combined stresses is the product of the aging rates under each single stress. *E, M, T,* and *L* are the electrical, mechanical, thermal, and lifetime factors. E_0 and M_0 are the scale parameters for the lower limits of the stresses and L_0 is the lifetime at these lower limits.

When dealing with the aging of insulating materials, subjected to thermal, electrical, and mechanical stresses, the Weibull function was used. Determining the likelihood of failure $P(L)$ at given stresses is compared with the shape parameter α. This can be seen in Equation 19, where $L_{63\%}$ is the failure time for the failure probability of 63% as a function of lifetime *L*. This Weibull function works well with stochastic accidents according to Zhang and Gockenbach’s research.

$$P(L) = 1 - \exp\left[-(L/L_{63\%})^{\alpha}\right] \tag{19}$$

When combining stresses, the probabilistic failure becomes denoted by Equation 20. In this function, the influences of thermal, electrical, and mechanical stresses have been substituted into the model. It can be seen that each term has an exponential impact on reliability. This model is more robust as it takes into account the system stresses.

$$P(L)=1-\exp\left[-\left(\frac{E}{E_0}\right)^{\alpha(n-bT)}\left(\frac{M}{M_0}\right)^{m\alpha}\left(\frac{L}{L_0}\right)^{\alpha}e^{\alpha BT}\right] \tag{20}$$

When applied, the models that Zhang and Gockenbach (2007) provide a means of connecting physical and statistical processes of component failures. Their approach was deemed useful to assess the reliability of a component, as well as clarify the causes of the failure. Of all the models created, time-dependent failure rate demonstrated the most significant results. The results from this model showed the dependency of the failure rate on component age and on the maintenance history. Their work also determined that different components had different significance of system stresses. Components such as transformers and housing were impacted by temperature. Zhang and Gockenbach (2007) state that in practice each failure can be activated in a defined usage interval, and that components can have different failure modes depending on time. Due to this a time-step mixture of the reliability model could potentially result in a better model of the failure rate.

2.8 Accelerated Life Testing

Accelerated life testing is a common practice for determining component or system reliability, while using conditions that differ from operating conditions. This in generally done due to cost and time constraints of the experiment. In some cases a component can have a very long life at its operating stress, and this in turn would make analyzing this in the form of an experiment time consuming. To bypass this, the same experiment is run at stresses higher than that of the operating stresses. This, in theory, yields a shorter time to failure therefore reducing the time of the experiment.

The two primary analytical components in accelerated life testing are a life distribution and a life-stress model. Failure data from the experiment is used to estimate the parameters of the life distribution. It is also important to fit the correct distribution to the failure data. This distribution can vary depending on the type of component as well as the types of stresses involved. Some of the common distributions used for accelerated life testing include: Weibull, exponential, normal, or Gaussian.

Life-stress relationships are used to relate test conditions to the operating conditions. There exist a multitude of different types of life-stress models, some of the common being: general-log linear, Eyring model, and Arrhenius model. Each of these has a specific application and should be applied situationally. The Arrhenius model, for example, is commonly used for accelerated life tests that involve temperature as the stress. In the case of this research the general log-linear approach is used. This is due the fact that it allows for a vector of stresses to be used. The relationship can be seen in Equation 21. It can be seen that the $\alpha_,$ coefficients in the equation are the model parameters, where X is a vector of stresses. This allows for a different degree of impact depending on the stress. It is this key factor that gives the general log-linear its versatility.

$$L\left(\underline{X}\right) = e^{\alpha_0 + \sum_{j=1}^{n} \alpha_j X_j} \tag{21}$$

A primary goal of this research is determining reliability of a component at a different, and more stressful, state. Research done by Mettas (2005) analyzed usage data to create predictive models. In his work he posed the question: “How do I utilize my customer’s usage data information?” He states that there are different types of customer usage data, each requirement needs a different treatment. Mettas (2005) explains that depending on the customer, the stress applied to the system or component can vary. From this, a usage profile can be developed and applied to models.

In his work Mettas (2005) analyzed a motor that experienced three distinct loads based on customer usage. The loads experienced by the motor were 6, 8, and 12 pounds. Failure data was collected for each operating condition and was recorded in terms of cycles-to-failure. From this a Weibull probability plot was developed, as can be seen in Figure 6. Each line indicates a different stress level. The use stress is a separate stress defined by Mettas and has a value of 7. The Weibull-inverse Power model was fitted to the failure data, and the respective parameters were estimated.

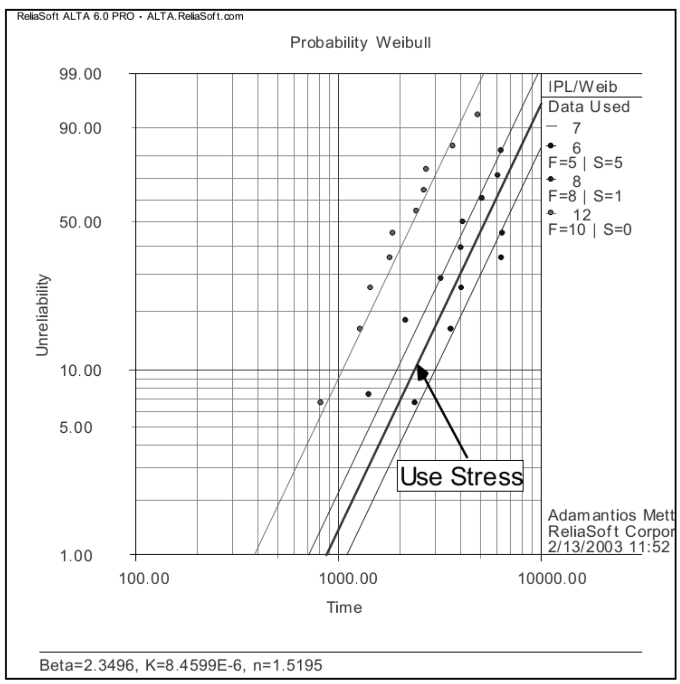

Figure 6: Weibull Plot for Multiple Stresses (Mettas, 2005)

After constructing the model using test data, customer surveys were conducted to determine the actual stress levels customers used. This differs from traditional experimentation, that would have used a mean of the test stresses. The values of this survey allowed for the creation of a revised model, whose pdf can be seen in Figure 7. This revised model and use stress allowed for more accurate predictions of the motors reliability.

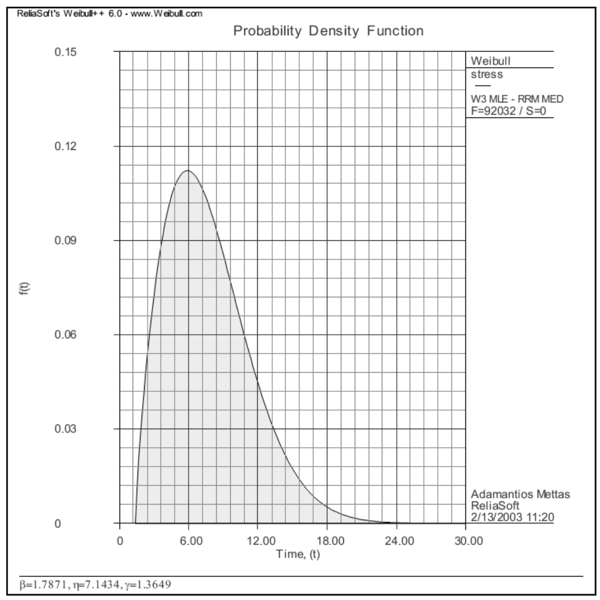

Figure 7: pdf Based on User Stress (Mettas, 2005)

2.9 RAMS Conference Submissions

Research conducted by Hada et al (2011) focused on system reliability models with changing load profiles. Their research was the ground work for this thesis and was submitted to the 20111 RAMS conference. In their work Hada et al sought to create reliability models as a function of system stresses. The goal was to predict reliability based on predicted future state stresses.

Johnson et al (2012), utilized concepts in this thesis in their research submitted to the 2013 RAMS conference. In this submission they used constrained maximum likelihood optimization to develop covariate based reliability models. The primary focus of their submission was the development of the modeling techniques.

3.0 Research Plan

The following sections outline the details of research conducted pertaining to this thesis. These topics include: construction of reliability models, reliability predictions, and model building processes. Work done in these areas was done in regards to research conducted with NAVAIR. Models and techniques used were applied to situations and datasets provided by NAVAIR.

Data for Navy Components/Systems

Currently in the Navy there exist two main information sources for catapult data: ASRL and logbooks. ASRL is a database that contains the launch information for every aircraft that is launched from the carrier. The information recorded includes aircraft type, weight, and end speed. Information is collected electronically and immediately stored within the system. The weight of the aircraft includes both the aircraft itself, as well as its payload. The end speed is the speed of the aircraft before separation from the catapult.

Logbooks are the maintenance logs kept by the carrier's crew. These contain all the maintained actions performed, and give a detailed explanation of the actions performed. Logbooks have been mined for failure data, which was then stored in a database. This database allows for instantaneous access to failure data for any catapult component. This information is critical in developing reliability models for the components under study.

Software

Software used to estimate parameters, as well as make reliability predictions, have been provided by Reliasoft. The Reliasoft software suite specializes in software used for reliability analysis and accelerated life testing. Software included in this suite include: Weibull++, BlockSim, and ALTA. These different software packages each specialize in a different aspect of reliability analysis. Weibull++ is used for fitting distributions to reliability data that is not stress dependent. Stress-based models are be made with the aid of ALTA. This software processes failure data that has corresponding stresses. The models that ALTA creates are a function of use stresses, or system stresses. Both programs allow for the fitting of various distributions. BlockSim is software that allows for the creation of reliability-based system simulations. Together, these different software packages allow for a complete reliability analysis of a system or component.

3.1 Previous Work

Preliminary models to describe system reliability, with respect to system stresses, have produced mixed results. These models were the building blocks to the approach outlined in this research. The models developed include using mean aircraft weight, mean end speed, mean stresses and respective standard deviations, and a percentile based approach.

The general approach for these models is based on the Weibull distribution. This is done because of the general behavior of the system. Mechanical systems that experience an increasing failure rate are often described by a Weibull distribution. Historically their usage has been successful when applied to failure data of these systems. The Weibull model used is the two parameter distribution. Due to limited data, the estimation of additional parameters is not advisable or in this case necessary, making the selection of the three parameter Weibull not favorable. In these approaches, the stresses believed to impact reliability are addressed in the scale parameter of the distribution. By making the scale parameter a function of these stresses, they can potentially have an impact on reliability of the component. The shape parameter is not a function of stresses however; doing so would imply a change in failure mode. This general approach can be seen in Equation 22. The *x* terms in the model are the system stresses and the values of α and β are estimated from the failure data. Stress values are input into the model and determined by usage profiles. In practice, a negative value of an α_j term indicates a negative impact on reliability. A positive value for an α_j term indicates that the stress does not impact the model or it improves reliability. This outcome generally implies that the data cannot accurately describe the failure in terms of the respective stress.

$$\begin{aligned}
&R(t) = e^{-\left(\frac{t}{\eta}\right)^{\beta}} \\
&\text{where:} \\
&\eta = \text{Scale Parameter} \\
&\beta = \text{Shape Parameter} \\
&\eta = e^{\alpha_0 + \alpha_1 x_1 + \alpha_2 x_2 + \ldots + \alpha_i x_i}
\end{aligned} \tag{22}$$

A model using mean weight was developed to factor in aircraft weight into the reliability model. This approach used a two parameter Weibull distribution, with the scale parameter as a function of mean weight. Equation 23 shows the general form of the reliability model. Requirements for this model included failure data, in which the mean weight for the respective failure interval was known. An illustration of this can be seen in Figure 8. Determining the mean weight for a given interval was done by cross-referencing a failure from logbooks with usage information from ASRL. Logbooks provided the installation and failure times and ASRL provided the aircraft weight for the launches in the interval. Once determined, the mean weight for the interval as well as the number of cycles were used as inputs into ALTA.

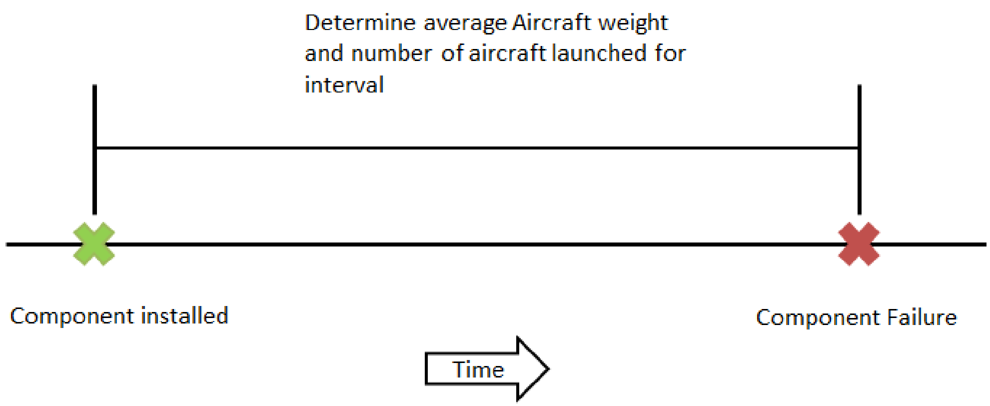

Figure 8: Failure Description

$$R(t) = e^{-\left(\frac{t}{\eta}\right)^{\beta}}$$

where:

$$\beta = \text{shape parameter}$$

$$\eta = \text{scale parameter} \tag{23}$$

$$\eta = e^{\alpha_0 + \alpha_1 \mu_{AW}}$$

The primary disadvantage of this approach was that it did not include end speed into the reliability model. This was a concern to in-service engineers, who deemed that this was an important factor. Because of this, a supplemental approach was created which factored in both weight and end speed. The general form of this model can be seen in Equation 24. In this model the Weibull scale parameter is a function of both weight and end speed.

$$
\begin{aligned}
&R(t) = e^{-\left(\frac{t}{\eta}\right)^{\beta}} \\
&\eta = e^{\alpha_0 + \alpha_1 \mu_{AW} + \alpha_2 \mu_{ES}}
\end{aligned}
\tag{24}
$$

Despite producing promising results, a model factoring in mean weight and end speed was deemed not entirely appropriate. This was due to the discovery that weight and end speed were correlated. Because of this, the confidence of the parameter estimation was reduced. In doing so it was decided that the model with mean weight and end speed was undesirable.

These simple models can be applied to any system or component that experiences recorded stresses and failures. The application is not limited to aircraft carrier components by any means. Furthermore these models can potentially be enhanced by adding the standard deviation of stresses to the model. In some cases a high variation in stresses could lead to a decrease in system of component reliability. An example of this model can be seen in Equation 25.

$$
\begin{aligned}
&R(t) = e^{-\left(\frac{t}{\eta}\right)^{\beta}} \\
&\eta = e^{\alpha_0 + \alpha_1 \mu + \alpha_2 \sigma} \\
&\text{where:} \\
&\mu = \text{mean weight} \\
&\sigma = \text{weight standard deviation}
\end{aligned}
\tag{25}
$$

3.2 Classification of Stresses

Due to the correlation concerns involving mean weight and end speed, there existed a need for an alternative method for classifying launches while still using both stresses. This need was met with the introduction of binning, which grouped launches based on weight and end speed combinations. By grouping launches based on weight and end speed it was possible to indirectly factor in the two different stresses. This binning and classification can only be done with the aid of personnel knowledgeable with both the system as well as the stresses within the system. Bins cannot be arbitrarily made, and doing so would generate inaccurate results.

Data binning is a critical aspect in the model building process. The general idea of data binning is grouping similar system loads based on their respective stresses. By grouping multiple loads in a single bin it is implied that they all affect the system in a similar manner. The main advantage of grouping loads into bins is that it makes parameter calculations easier. The alternative to this approach would be to have every unique load factored into the reliability model separately. By reducing the number of loads, the number of respective covariates is reduced in the reliability model. Due to the limited data available, the binning approach makes model building and parameter estimation much more feasible.

Figure 9 represents a sample binning diagram, where each color represents a separate bin. It can be seen that bins are determined by their thresholds of two different stresses. In practice it is possible to have fewer or more stresses to determine bin groupings. If a certain load is within the bin thresholds it is considered to be part of that bin.

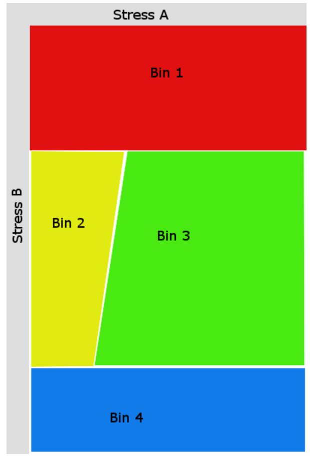

Figure 9: Binning Diagram

Mathematically each bin represents a percentage of the total number of loads seen in a given interval. This can be seen in Equation 26, where x_i is the percentage of loads in bin i. These bin percentages can then be used for reliability analyses. In the case of constrained optimization, these are the primary inputs into both ALTA and the reliability function.

$$x_i = \frac{\text{total number of loads in bin } i}{\text{total number of loads in interval}} \tag{26}$$

The application of bins in the reliability function can be seen in Equation 27. It can be seen that reliability model is a function of both bin percentages and time. The scale parameter of the two parameter Weibull is a function of bin percentages. Because of this, any shift in usage has an impact on component reliability.

$$R(t,x) = e^{-\left(\frac{t}{\eta}\right)^{\beta}}$$

where:

$$\eta = \exp(\alpha_0 + \alpha_1 x_1 + \alpha_2 x_2 + ... + \alpha_n x_n) \tag{27}$$

x_i = relative frequency of bin i

n = number of bins

3.3 Constrained Maximum Likelihood Optimization

The general purpose of this approach is to create a stepwise approach to model building in which the data itself determines the optimal form. This approach uses the two parameter Weibull distribution, with the scale parameter a function of stress. The stresses of the system use a binning-based approach. They must be similar and able to be grouped. If the system stresses cannot be binned, this approach is not valid and cannot be used. It is also important to note that an initial set of bins must be defined prior to this approach. This process does not aid in the initial creation of bins. Also, it is vital to understand the relationship between bins. By this it is meant that the relative impact from one bin to another must be known. In this section's example, for instance, it is known that relative bin stress increases in ascending bin order. Other cases it might be the reverse, but it still must be taken into consideration. Without this knowledge it is impossible to properly use this technique. Figure 10 shows the general flow of the process.

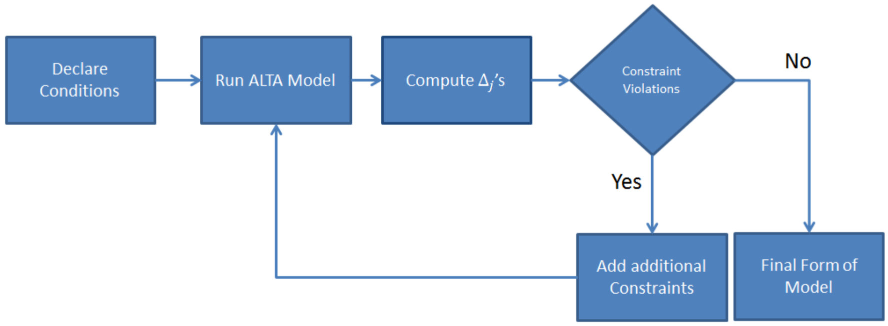

Figure 10: Constrained Process Flow

3.3.1 Model and Constraints without Baseline

It is important to first declare the objective and constraints of the model. One key point to note is without the use of a baseline the α_j coefficients do not have to be negative. Instead they should follow the constraints shown in Equation 28. The general concept of these constraints is that the α_j values must have descending values. This is because historical information for this example indicates that as bins ascend the relative stress increases. These constraints are the basis on which the entire approach is based on. The number of α_j terms, *n*, in the initial constraints is equal to the number of initial bins created.

$$
\begin{array}{ll}
\text{Max} & L(\underset{\sim}{\alpha}) \\
\text{st} & \alpha_1 \geq \alpha_2 \\
 & \alpha_2 \geq \alpha_3 \\
 & \ldots \\
 & \alpha_{n-1} \geq \alpha_n \\
 & \underset{\sim}{\alpha} = (\alpha_1, \alpha_2, \alpha_3, \ldots, \alpha_n)
\end{array}
\tag{28}
$$

It is also worth noting that the α_j terms in Equation 28 are related to the two parameter Weibull function, which is illustrated in Equation 29. The value of α_j indicates the impact a given bin has on component reliability.

$$
\begin{aligned}
&R(t) = e^{-\left(\frac{t}{\eta}\right)^{\beta}} \\
&\text{where:} \\
&\eta = \eta_0 \exp(\alpha_1 x_1 + \alpha_2 x_2 + ... + \alpha_n x_n) \\
&x_i = \text{relative frequency of bin } i
\end{aligned}
\tag{29}
$$

Step 1: Initial Run

Step 1 involves solving the ALTA model without the usage of constraints. By this it is meant that the model is run with every parameter, or in this case bin, being used. This outputs all of the necessary information to evaluate the constraints outlined in Equation 28. Table 1 shows a sample output of alphas for a binning scenario with *n* bins. It can be seen that each bin has a corresponding α_j. In the event that the model does not run when attempting to estimate *n* alpha values, a different approach using a baseline must be used. This approach is outlined in Section 3.3.2 of this document.

Table 2: Alphas from Initial Run

Bin 1	Bin 2	Bin 3	…	Bin *n*
$\propto_1$	$\propto_2$	$\propto_3$	…	$\propto_n$

Compute Constraint Violations

After the completion of Step 1, the outputted alphas are used to compute the constraint violations. These violations show to what extent the alphas digress from the given rules. Equation 30 outlines the process for computing constraint violations. By this it is meant that the difference between each set of alphas is computed. This approach holds true for any binning scenario; however the number of violations computed would change.

$$\begin{aligned}&\Delta_l = \alpha_{l+1} - \alpha_l \\ &\text{for } l = (1, 2, 3, \ldots) \\ &\text{where } l = \text{toal number of bins-1}\end{aligned} \tag{30}$$

Determine the Highest Constraint Violation

Once all of the constraint violations have been computed the next step is to find the largest value of Δ_l. This can be seen mathematically in Equation 31. The rationale behind this is that the largest Δ_l is causing the most damage to the model. By finding the maximum Δ_l it is possible to locate the cause; α_l. The corresponding alpha parameter is then renamed to avoid confusion. This can be seen in Equation 30.

$$\begin{aligned}&\max_l \Delta_l = \Delta_j \\ &j = k \\ &\alpha_j = \alpha_k\end{aligned} \tag{31}$$

Add Additional Constraint

The results of Step 3 indicate what bins must be addressed. Unlike other modeling techniques parameters cannot simply be eliminated from the model. Therefore, a different approach must be taken. This new approach is to combine the two bins that created the largest value of Δ_l. This is mathematically shown in Equation 32. The reason for this stems from the constraint violations. These violations indicate that ALTA cannot distinguish one parameter from the other. Because they cannot be differentiated the logical assumption would be to combine them.

$$\alpha_k = \alpha_{k+1} \tag{32}$$

These new alphas are applied to the reliability model in Equation 33. It can be seen that bins *k* and *k*+1 now share a common alpha value. This combination approach translates back into the original data set. By this it is meant that the failure data from bin *k* is added to bin *k*+1 to create a single bin. The failure data being combined is the percentages for each bin for the respective failure.

$$\eta = e^{\alpha_0 + \alpha_1 x_1 + \ldots + \alpha_k x_k + \alpha_k x_{k+1} + \ldots + \alpha_n x_n} \tag{33}$$

Step 5: Return to Step 1

Once the data set has been combined in the appropriate manner the entire process is repeated. This is done continually until there are no constraint violations or every bin has been combined. Once there are no violations the final form of the model has been obtained. In the event all the bins converge into one bin an alternative approach is needed. Such a scenario implies that the impact of each bin, in terms of reliability, is indistinguishable.

3.3.2 Model and Constraints (with Baseline)

The general approach to this method remains the same with the usage of a baseline. The selection of the baseline is important, and should be based on professional advice. The general theory of the baseline is to compare the impact of each bin to a selected bin. It is therefore most sensible to select the least stressful bin that contains loads in it. With the addition of the baseline comes the addition of constraints. These can be seen in Equation 34. It is shown that the addition of a baseline forces all alphas with a subscript greater than the baseline to be negative. Once these initial constraints have been created the remaining steps are the same for this method.

$$\begin{array}{ll} \text{Max} & L(\underset{\sim}{\alpha}) \\ \text{st} & \alpha_1 \geq \alpha_2 \geq \alpha_3 \geq \ldots \geq \alpha_n \\ & \alpha_1 \geq 0 \\ & \alpha_2 = 0 \\ & \alpha_3, \ldots, \alpha_n \leq 0 \\ & \underset{\sim}{\alpha} = (\alpha_1, \alpha_2, \alpha_3, \ldots, \alpha_n) \end{array} \tag{34}$$

A strength of this baseline approach comes from an intrinsic problem when estimating parameters using ALTA. Due to a lack of sufficient failure data, estimating every parameter of the model in the initial run is often times impossible. Doing so yields a system error thus making the approach outlined in Sections 3.3.1 impossible. The addition of the baseline bypasses this by never asking the software to estimate a complete set of model parameters.

3.4 Constrained Method Results

Upon receiving failure data from NAVAIR thorough analysis was conducted to understand the behavior of the data. These analyses included descriptive statistics, histograms, and time series plots. Histograms were created to understand the frequency of different stress levels for different time periods. The different time periods represent the time before and after additional squadrons of F-18E/F’s were added. The time study was conducted to determine if there was a noticeable shift in stress levels over time. After the completion of the preliminary tests, models were built using the failure data.

Histograms were created for multiple aircraft carriers deployed by the Navy, these include: CVN 74, CVN 75, CVN 76. For the purpose of this analysis CVN 75 is or primary importance. This is due to the fact that CVN 75 at this time has the most reliable failure data. The histograms created for this ship can be seen in Figures 11 and 12. Figure 11 represent the frequency of different aircraft weights before the additional squadrons of F-18E/F were added. From these histograms it can easily be seen that the additional squadrons has a noticeable impact on the distribution of weight. This outcome reinforces the statements from in-service that the additional squadrons had a noticeable impact in terms of weight. An additional set of histograms were created to analyze end speed. Despite the prediction that it too would show an increase after the addition of squadrons, there was not. This stress did not show any visible shifts post addition of F-18E/F's.

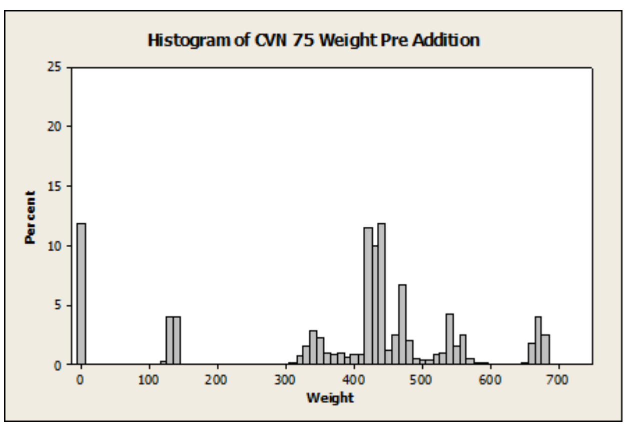

Figure 11: Histograms of Weight Pre-Addition

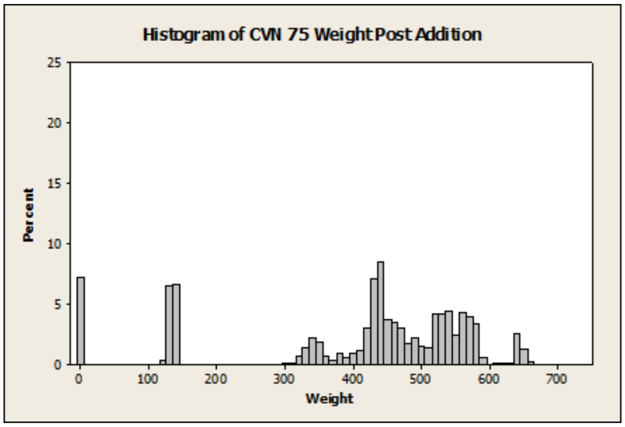

Figure 12: Histogram of Weight Post-Addition

Histograms were also created to analyze shifts in bin usage over time, which can be seen in Figures 13, 14, 15, and 16. Each graph represents a different catapult on CVN 75. Within each graph, bins are analyzed over three different time periods. This was done to understand the impact of air wing composition in pin usage. It can be seen that the most stressful bin is bin 7. It has a downward trend. Bin 6 however, has a much more pronounced upward trend. Form this it can be seen that the overall usage of more stressful aircraft increases over time.

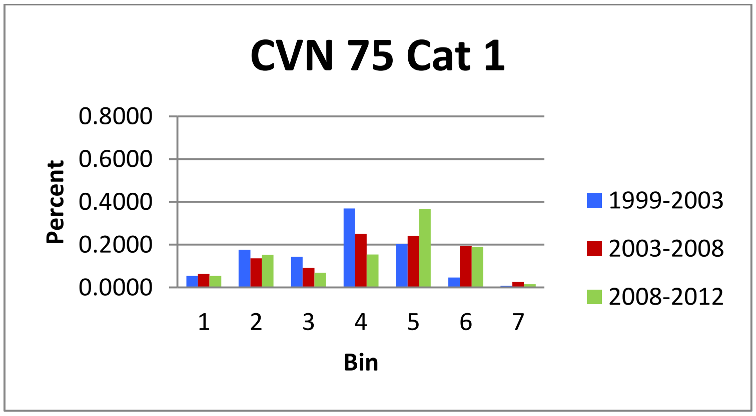

Figure 13: CVN 75 Cat 1 Bin Histogram

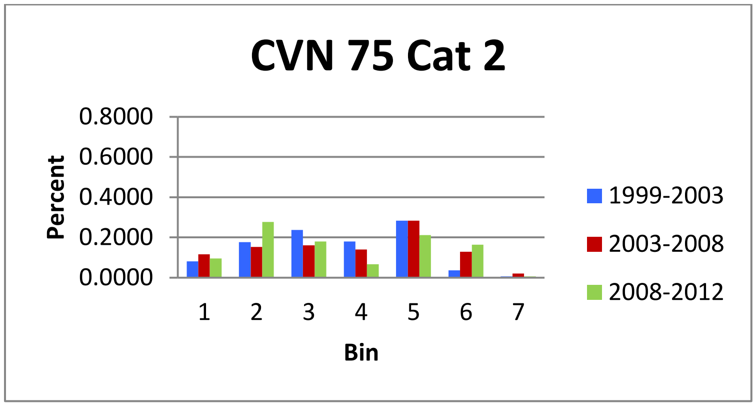

Figure 14: CVN 75 Cat 2 Bin Histogram

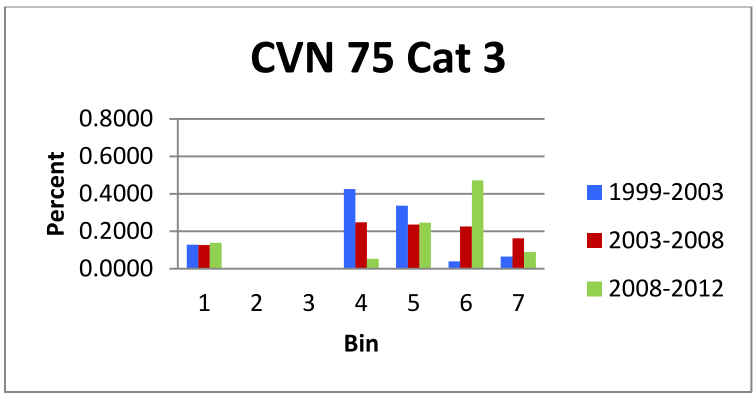

Figure 15: CVN 75 Cat 3 Bin Histogram

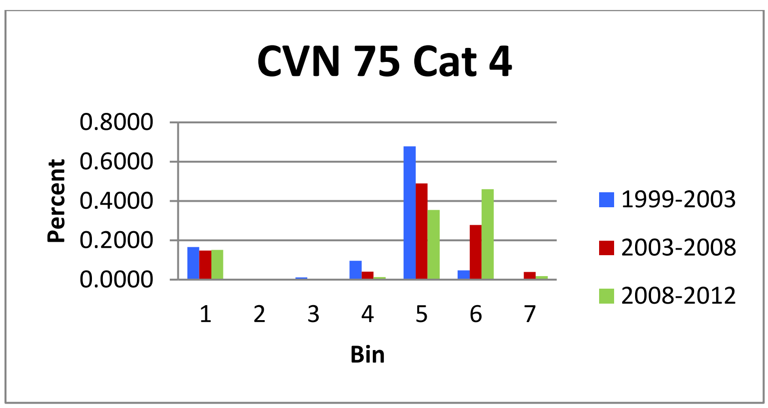

Figure 16: CVN 75 Cat 4 Bin Histogram

When modeling the failure data the constrained approach took precedence over models such as mean weight and end speed. In these models the initial binning classification had seven distinct bins. From these, the approach combined similar bins using failure data provided by NAVAIR. Components included in this study include nose gear launcher, bridle tensioner, water brake, and improved piston assembly. These components were selected due to the fact that they had failure data available at the time of this study. The baseline approach was used for this study, as the lack of a baseline led to errors in the initial step of the constrained approach.

The nose gear launcher successfully used the constrained approach and the results can be seen in Equation 35 and Table 2. Equation 35 shows the final form of the model, in which all but bins 6 and 7 have been combined into the base line. From this it can be concluded that only the most stressful bins have a negative impact on reliability. This model was then used to predict a future mean life, in cycles, based on an anticipated usage pattern. The results from this can be seen in Table 2. It can be seen that the more stressful future state, that has an increase in heavy aircraft, negatively impacts the reliability of the nose gear launcher.

$$\begin{gathered} R(t) = e^{-\left(\frac{t}{\eta}\right)^{\beta}} \\ \eta = e^{\alpha_0 - .592 x_6 - .592 x_7} \end{gathered} \tag{35}$$

Table 3: Mean Life Predictions for NGL

Time Period	Mean life (cycles)
2003 to 2008	583
2008 to 2012	554

The water brake also successfully utilized the constrained approach and produced similar results. The final form of the model can be seen in Equation 36. This model is slightly different in the sense that three bins have a negative impact on component reliability. In this model bins 5, 6, and 7 all impact component reliability in a negative manner. Bins 1 through 4 all have been combined with the baseline. Table 3 shows the mean life predictions for the future usage profile, and indicates that mean life is anticipated to decrease.

$$
\begin{aligned}
R(t) &= e^{-\left(\frac{t}{\eta}\right)^{\beta}} \\
\eta &= e^{\alpha_0 - 1.808 x_5 - 1.808 x_6 - 1.808 x_7}
\end{aligned}
\tag{36}
$$

Table 4: Mean Life Predictions for WB

Time Period	Mean life (cycles)
2003 to 2008	1134
2008 to 2012	1054

The bridle tensioner in a similar manner to that of the nose gear launcher completed the constrained approach. It also formed a model with two significant bins i.e., bins 6 and 7. This model can be seen in Equation 37. Mean life predictions were also made using this model and are located in Table 4. Once again the mean life is anticipated to decrease in the more stressful future state.

$$R(t) = e^{-\left(\frac{t}{\eta}\right)^{\beta}}$$
$$\eta = e^{\alpha_0 - .537 x_6 - .537 x_7} \tag{37}$$

Table 5: Mean Life Predictions for BT

Time Period	Mean life (cycles)
2003 to 2008	846
2008 to 2012	808

Unlike the previous components the improved piston assembly was not able to use the constrained approach. This is most likely due to insufficient failure data for the component. This component had the least failure data collected when compared to the others. Because of this a simple Weibull model was fit to the failure data. The results of this can be seen in Table 5.

Table 6: Parameters for IPA Weibull Model

Beta	Eta	LK
.819	666.8	-283.33

Summary of results

The results of the constrained approach have proved that the algorithms used can produce working reliability models. In all but one case there were successful in estimating the parameters necessary for an applicable reliability model. The method was also able to determine if the reliability model was not an appropriate fit for the data. This was evident in the case of the improved piston assembly, which failed to conform to the constraints of the algorithm. These models that the constrained approach has generated form the groundwork of further reliability assessments.

4.0 Parameter Estimation Utilizing Constrained Nonlinear Optimization Search

An alternative approach to using ALTA is to use Excel to find the optimal set of model parameters as well as bin groupings. This can be done by correctly applying the nonlinear optimization tools supplied in the Excel solver package. This software package has the ability to compute nonlinear optimization. While the algorithm is not exactly the same as ALTA, the estimation process is similar.

The purpose of estimating the parameters in an entirely new approach has two main benefits. Firstly, it allows for the verification of the parameter estimations that ALTA provides. In theory, both approaches should have similar results for the α_j parameters of the scale parameter. This is in part because the Excel method is subject to the same constraints as the ALTA model. The estimation is also derived from the same data set and the reliability model being used remains the two-parameter Weibull. Slight discrepancies are to be expected however. This is due to the fact that ALTA and Excel utilize different optimization algorithms.

The second benefit is that this approach is completely automated, that is to say that the grouping of the bins is not a manual process. Results from the Excel process that agree with the manual ALTA process would indicate that the stepwise process of the constrained method did not negatively affect the model. A possible drawback to using the constrained approach is that the linear approach to the combinations of bins bypasses a superior model. Because the Excel method blindly searches for the optimal model, it is possible that this method could find a different optimal solution.

Approach

The general approach to this method is the same as the approach outlined for constrained likelihood estimation; however it is automated by means of nonlinear optimization. The constraints previously outlined remain the same, and are used in the nonlinear optimization process. Equation 38 shows the constraints used for the optimization process. It can be seen when compared to Equation 28 that they remain the same. The constraints used in both methods indicate that as the value of *n* increases, the value of the respective α_j term should decrease. This stems from the fact that the corresponding bin stress increases as the value of *n* increases. These constraints are implemented by the comparison of cell values in Excel and are not explicitly stated in the spreadsheet.

$$\begin{aligned} &\alpha_1 \geq \alpha_2 \\ &\alpha_2 \geq \alpha_3 \\ &\ldots \\ &\alpha_{n-1} \geq \alpha_n \\ &\underset{\sim}{\alpha} = (\alpha_1, \alpha_2, \alpha_3, \ldots, \alpha_n) \end{aligned} \tag{38}$$

The objective function for the nonlinear optimization is the log-likelihood function. Due to the nature of the problem, it is in this case easier to work with the natural logarithm of the likelihood function. Equation 39 shows the objective function for the optimization process. It can be seen that the objective function is the sum of the logarithm of the pdf at each failure time. For the purposes of this application, the objective function is maximized. At the optimal maximum solution, the correct parameters are obtained. This objective function is subject to the constraints outlined in Equation 38. Similar to the constraints, this equation is not visible in the spreadsheet and is instead imbedded in a specified cell.

$$\begin{aligned}&\max \ \sum_{i=1}^{n} \ln\left(f_i(t_i)\right)\\&where\\&n = \text{number of failures}\end{aligned} \tag{39}$$

The combination of the objective function and constraints can be seen in Equation 40. This is the backbone of the optimization process and what is inputted into Excel. When inputted, the constraints and objective function take on a slightly different from however. The constraints in the equation are imbedded in the Excel solver function and the objective function is imbedded in a cell. This format can be applied to any component, given that there is failure data with the necessary stress data.

$$\begin{aligned}&\max: \ \sum_{i=1}^{n} \ln\left(f_i(t)\right)\\&st\\&\qquad \alpha_1 \geq \alpha_2\\&\qquad \alpha_2 \geq \alpha_3\\&\qquad \ldots\\&\qquad \alpha_{n-1} \geq \alpha_n\\&\qquad \underset{\sim}{\alpha} = (\alpha_1, \alpha_2, \alpha_3, \ldots, \alpha_n)\end{aligned} \tag{40}$$

4.1 Optimization Spreadsheet

An Excel spreadsheet was created to compute the nonlinear optimization. This spreadsheet can be seen in Figure 17. Spreadsheets were created for each of the primary catapult components; nose gear launcher, improved piston assembly, bridle tensioner, and water brake. All the necessary information used in the nonlinear optimization process is contained in these spreadsheets. Cells in the CTF column are the recorded failure times in cycles. Columns labeled X1 through X7 are the bin percentages for each corresponding failure. These data fields are populated from collected failure data and are not variables.

The scale parameter column, η, is calculated for each individual failure. This parameter is a function of bin percentages and the α_j values. This is illustrated mathematically in Equation 41. Because the scale parameter is a function of the alpha values, its value changes throughout the optimization process. The pdf is also calculated for each individual failure and the equation for this is shown in Equation 42. From pdf column the natural logarithm of the pdf is computed in a separate column. The column of natural logs of the pdf's is then summed; this is the objective function for the optimization process. This summation is located in the cell labeled "sum".

IPA											
β	α0	α1	α2	α3	α4	α5	α6	α7			
1.080	7.821	4.487	0.000	0.000	0.000	0.000	0.000	-6.510			
	CTF	X1	X2	X3	X4	X5	X6	X7	η	f(t)	ln(f(t))
	72.000	0.042	0.000	0.000	0.944	0.014	0.000	0.000	3.0130546032E+03	2.6120701093E-04	-8.2501973197E+00
	2321.000	0.061	0.206	0.098	0.469	0.122	0.042	0.002	3.2285601938E+03	1.6175993482E-04	-8.7293972057E+00
	6130.000	0.054	0.119	0.092	0.200	0.301	0.203	0.031	2.5919544661E+03	3.5429923729E-05	-1.0247953792E+01
	2317.000	0.071	0.000	0.003	0.199	0.170	0.495	0.062	2.2957986882E+03	1.7146748042E-04	-8.6711169279E+00
	7189.000	0.038	0.202	0.091	0.156	0.375	0.122	0.016	2.6666231074E+03	2.3682057665E-05	-1.0650792857E+01
	764.000	0.116	0.000	0.431	0.088	0.302	0.048	0.014	3.8279985694E+03	2.0809834120E-04	-8.4774997958E+00
	770.000	0.055	0.378	0.299	0.029	0.217	0.023	0.000	3.1839094074E+03	2.4400007458E-04	-8.3183420270E+00
	879.000	0.076	0.304	0.279	0.061	0.174	0.100	0.006	3.3815997949E+03	2.2705810874E-04	-8.3903045876E+00
	3732.000	0.140	0.000	0.001	0.125	0.194	0.338	0.201	1.2628366084E+03	3.7157966323E-05	-1.0200332373E+01
	861.000	0.103	0.000	0.000	0.028	0.125	0.459	0.285	6.2172793267E+02	4.3035940038E-04	-7.7508898835E+00
	55.000	0.055	0.000	0.000	0.018	0.127	0.564	0.236	6.8344093041E+02	1.2095016073E-03	-6.7175468990E+00
	186.000	0.134	0.000	0.000	0.054	0.102	0.457	0.253	8.7938564775E+02	8.9980408878E-04	-7.0133334975E+00
	186.000	0.134	0.000	0.000	0.054	0.102	0.457	0.253	8.7938564775E+02	8.9980408878E-04	-7.0133334975E+00
	4229.000	0.136	0.000	0.002	0.053	0.496	0.284	0.028	3.8340829171E+03	9.3404778612E-05	-9.2785680512E+00
										sum	-1.1970960871E+02

Figure 17: Excel Worksheet

$$\eta = e^{\alpha_0 + \alpha_1 x_1 + \ldots + \alpha_7 x_7} \tag{41}$$

$$f(t) = \frac{\beta}{\eta}\left(\frac{t}{\eta}\right)^{\beta-1} e^{-\left(\frac{t}{\eta}\right)^{\beta}} \tag{42}$$

Multiple cells in this spreadsheet are variables that change as the optimal solution is determined. The columns CTF and X1 through X7 are constants that do not change for a particular failure event. The data for these columns are collected from logbooks then inputted into the spreadsheet. The values of the α_j parameters are decision variables for the nonlinear optimizations. In the initial stage these values are nominally set to zero. β is also a decision variable and changes as the optimal solution is determined. In the initial stage this parameter is set to 1. The initial values for the α_j parameters and shape parameter give the optimization process a starting location. η and the pdf are functions of the previously mentioned terms..

Constraints are not explicitly stated in the spreadsheet. Instead they are declared in the solver function. These constraints are outlined in Equation 38, but can be seen in

Figure 18. In this each cell represents the corresponding alpha term for the given constraint. Figure 19 also shows the selected cells for the decision variables. For this nonlinear optimization, the alpha parameters are the decisions variables. In previous iterations of this method β was also a decision variables, however this led to problems in the optimization process. By having the α_j parameters the decision variables it allows for this approach to both estimate the distribution parameters as well as groups bins. After the optimization is run, any bins with the same alpha values are considered to be combined. This grouping essentially the same as the constrained approach, however the grouping is automated and does not require human intervention.

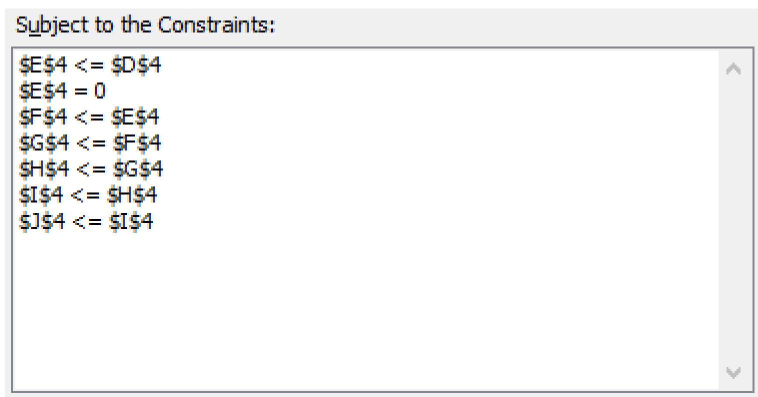

Figure 18: Excel Constraints

α0	α1	α2	α3	α4	α5	α6	α7
7.821	4.487	0.000	0.000	0.000	0.000	0.000	-6.510

Figure 19: Decision Variables

4.2 Comparison Analysis

A comparison of results collected from ALTA and Excel was performed. The purpose of this was to determine if the α_j parameters have similar values as well as if the bins have similar groupings. Results were collected for the NGL, IPA, BT, and WB from both methods. Tables were created to illustrate the comparison of areas of interest. Reliability predictions for each method were computed to determine if there was a significant difference in each method's results.

Nose Gear Launcher

Table 6 contains the outputs from both the Excel and ALTA approaches. Both approaches were able to create final models that adhere to the model constraints. It can be seen that the groupings of bins are identical. This implies that the bins that were created by the ALTA grouping algorithm were replicated with the nonlinear optimization in Excel. This is an important finding as it gives significant credit for the optimal bin groupings. The α_j values for both outputs are similar, although there is a small discrepancy. This difference can possibly be attributed to the different optimization algorithm used by the methods. It is also important to note that all alpha values are negative, a requirement to have a meaningful model.

Table 7: NGL Outputs

Alpha	α0	α1	α2	α3	α4	α5	α6	α7
Excel	6.661	0	0	0	0	0	-.690	-.690
ALTA	6.328	0	0	0	0	0	-.592	-.592

Table 7 shows how reliability predictions differ for each model and a percent difference was computed. A reliability prediction was done at 500 cycles for each method and bin percentages were based on current aircraft usage. The results indicate that the ALTA model generates more pessimistic results than that of the Excel model. The difference between the two predictions is also greater that for other components. The difference in the alpha parameter estimation is amplified, as it is an exponential term in the reliability model. Despite this the methods did not create reliability predictions that varied in an extreme manner.

Table 8: NGL Comparison

	R(500)
Excel	.556
ALTA	.453
% Difference	18.4%

Improved Piston Assembly

The results for the Improved Piston Assembly are located in Table 8. Both of these approaches produce results indicating that this data set could not produce a complex model. Both the Excel and ALTA version's final models produced final models with extremely negative α_j terms. α_7, in both cases, was found to be too negative to be realistic. The Excel version also returned an extremely positive value for bin 1's α_j parameter. In terms of caparison these results are beneficial. The two approaches came to the same conclusion that the data could not be modeled as a two parameter Weibull with covariates.

Table 9: IPA Outputs

Parameter	α0	α1	α2	α3	α4	α5	α6	α7
Excel	7.821	4.486	0	0	0	0	0	-6.510
ALTA	8.004	0	0	0	0	0	0	-5.41

Bridle Tensioner

In the case of the bridle tensioner, both approaches created working models in their final iterations. The results from the Excel and ALTA approaches are located in Table 9. This final model, in both cases, has bins 6 and 7 grouped together. This is an important finding as it shows that the nonlinear optimization and manual groupings came to the same conclusions. These results are similar to that of the NGL which also had an agreement with both methods. It can also be seen that the α_j values are similar in magnitude. There is a slight difference, however this could be attributed to different optimization algorithms. These results are still favorable as the α_j values do not vary greatly between the two methods.

Table 10: BT Outputs

Parameter	α0	α1	α2	α3	α4	α5	α6	α7
Excel	6.987	0	0	0	0	0	-.638	-.638
ALTA	6.723	0	0	0	0	0	-.537	-.537

A comparison of reliability was done for the two models. Reliability predictions were made and compared at a time of 500 cycles and results can be seen in Table 10.

Values for bin percentages were created form the average values found in real failure data. These results indicate approximately a 10% difference in reliability estimation. This difference is much lower than the differences computed for the nose gear launcher, which had an 18.4% difference. It can be seen that the ALTA reliability prediction is more pessimistic than that of the Excel model. This stems from the varying α_j values that were computed.

Table 11: BT Comparison

	R(500)
Excel	.644
ALTA	.576
% Difference	10.6%

Water Brake

The Water Brake data also produced similar results for both the Excel and ALTA methods. The results from the Excel and ALTA methods are located in Table 11. The final form of each model conformed to the requirements for a working model. All α_j values were negative and in descending magnitude. In each case bins 5 through 7 were combined into a single bin. Bins 1 through 4 were also combined into a baseline bin. These results are similar to previous results including the NGL, and IPA in which both methods produced the same binning combinations. While the α_j values are not as close as previous components, they do not differ greatly.

Table 12: WB Outputs

Parameter	$\alpha0$	$\alpha1$	$\alpha2$	$\alpha3$	$\alpha4$	$\alpha5$	$\alpha6$	$\alpha7$
Excel	7.96	0	0	0	0	-1.808	-1.808	-1.808
ALTA	7.69	0	0	0	0	-1.081	-1.081	-1.081

The reliability predictions for the water brake can be seen in Table 12. It can be seen that these predictions are much closer than previous components. The difference in reliability is under one percent, which is a significant finding. This difference in reliability estimation is much lower than the nose gear launcher and bridle tensioner, which had differences of 18.4% and 10.6% respectively. Such a small difference indicates that this model and approach fits the data extremely well. From this it can be concluded that both methods create the same bin groupings as wells as extremely close reliability predictions.

Table 13: WB Comparison

	R(500)
Excel	.701
ALTA	.697
% Difference	0.55%

4.3 Comparison Results

From this comparison it is evident that both approaches yield similar results. In all cases both approaches grouped bins in an identical manner. Similarly, α_j values for both approaches were found to be quite similar. The only component that had significantly different α_j values, the IPA, could not create a working model for either method. Furthermore reliability estimations using the same bin percentages and cycle values yielded similar results. The estimated reliability was found to be reasonably close for all components that produced a working model. The results of this comparison imply that the algorithm used in the constrained approach, using ALTA, produces similar results to that of nonlinear optimization. Furthermore it indicates that the manual process of grouping bins does not negatively impact the final results of bin groupings.

5.0 Future Possible States

Due to the nature of the system, there exist multiple possible future states of system stresses. By this it is meant that the loading profile at a future time is not known with absolute certainty. There are however, known possible future states that could potentially exist. These are known from historic information, known mission profiles, and anticipated changes in air wing composition. Changes in air wing composition are caused by the phasing out of older aircraft, as well as the addition of more combat specific aircraft. These possible profiles can be used in determining the possible future state reliabilities by quantifying them as inputs into the created reliability models.

These future states can be simulated to determine their impact on system performance. Currently within NAVAIR there exists concern that the addition of heavy aircraft, along with combat operations, could significantly decrease the operational reliability of the carrier catapults. Another concern expressed by NAVAIR is that their current maintenance polices will not be able to address the increase in system failures. By creating system level simulations, rather than single components, analyses can be conducted to assess the overall reliability. These simulations are able to determine if there are negative impacts on system reliability, as well as if the current maintenance policies can maintain system operation.

Simulation Software

To simulate the launcher system, BlockSim, a Reliasoft software, was used. This software allows for the simulation of multi-component systems whose reliability can be expressed mathematically. BlockSim also allows for integration with ALTA, thus allowing for the direct implementation of reliability models. The software is capable of determining availability, number of failures, criticality, as well as maintenance policies. For the purposes of this study, mean time to failure and number of system downing events are of primary concern. These two factors will show if the changes in stress profiles directly impact system reliability.

5.1 Simulation Approach

The catapult system is comprised of four primary components, all of which have been previously addressed in Section 1.2. These components include the nose gear launcher, bridle tensioner, improved piston assembly, and water brake. Because each of these is critical to the operation of the system, the system can be considered to be series in nature. Figure 20 illustrates this series system. From this it can be concluded that if any component fails it causes an entire system failure.

The reliability of these components can be determined by their respective reliability models. These were created using the constrained approach, and verified using the Excel method. Each component has a unique model, but all experience the same stress values. Equations 43 through 46 show the reliability models for each component. These equations, along with the known future stresses, enable for the determination of future state reliability.

The simulation has multiple assumptions that make the application of modeling techniques easier. Firstly, corrective actions are assumed to be deterministic. This is primarily due to the fact that a record of repair times is not available. Also, the repair time and availability of the system is not of primary concern. The main point of interest is the impact of the stress profile on reliability. The second assumption is that there exist a set number of future states. By this it is meant that there is not a continuous distribution of future state stresses. This assumption makes the modeling process much simpler. Instead of a continuous spectrum, a set of probable states will be simulated. Having a continuous state distribution would be extremely difficult using the available software packages. Lastly for the initial simulation, preventative actions are be ignored. This is because in this initial simulation the goal it to solely determine the impact of system stresses on component reliability. By adding in preventative maintenance actions the impact of system stresses can be hidden. A supplement simulation, that includes and analyzes preventative actions, is located in Section 6.

The final goal of the simulation approach is the creation of optimal maintenance polices. These are based on the results of the simulations run for each future state. After each scenario is run, an optimal maintenance policy is created. This policy will attempt to complete a preventative maintenance action before a corrective action must be performed. Such policies can be created within the Blocksim software. After maintenance policies have been created for each possible future state, they are weighted based on the probability of the respect states occurrence. This weighing action creates a generalized maintenance policy that will be effective for the possible future states.

Blocksim Model

The model for the Blocksim simulation can be expressed as a four component series system. This model can be seen in Figure 20. Each of the blocks in the figure represents a component in the system. Within each block resides the respective information of the component. Reliability models were directly imported from ALTA for each component. Corrective maintenance polices were also inputted for each component.

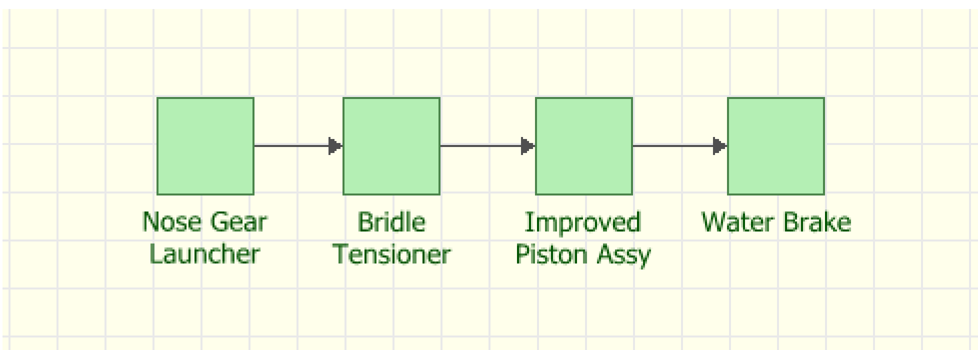

Figure 20: Blocksim Model

The reliability models for each component can be seen in Equations 43 through 46. These represent the optimal models found using the constrained approach and verified using the Excel approach. It can be seen in Equation 43 that the model for the IPA does not contain any covariates. This is because the IPA failed to produce a model using both the constrained and Excel methods. A simple two-parameter Weibull model was created as an input into the model.

$$R_{IPA}(t) = e^{-\left(\frac{t}{1868}\right)^{.732}} \tag{43}$$

$$R_{NGL}(t) = e^{-\left(\frac{t}{e^{-(6.72-.592x_6-.592x_7)}}\right)^{.729}} \tag{44}$$

$$R_{WB}(t) = e^{-\left(\frac{t}{e^{-(6.72-1.081x_5-1.081x_6-.1.081x_7)}}\right)^{1.077}} \tag{45}$$

$$R_{BT}(t) = e^{-\left(\frac{t}{e^{-(6.72-.537x_6-.537x_7)}}\right)^{.762}} \tag{46}$$

5.3 Future States

The stresses seen by the catapult system are directly related to the air wing composition and mission profiles of the aircraft carrier. It is known by NAVAIR that both of these are variable in nature and will change with time. Future air wing composition is known to with a certain degree of certainty and is predicted to have an upward shift in heavy aircraft. Mission profiles on the other hand are not known with exact certainty. Based on known information, four possible future states have been created. These future states are shown in Table 13.

Table 14: Future Stress States

	Bin 1	Bin 2	Bin 3	Bin 4	Bin 5	Bin 6	Bin 7	P_i
State 1	.05	0.15	0.1	0.25	0.10	0.2	0.2	.15
State 2	0.05	0.1	0.1	0.15	0.10	0.3	0.2	.35
State 3	0.1	0	0.05	0.1	0.15	0.30	0.25	.20
State 4	0.05	0	0.05	0.1	0.15	0.35	0.30	.30

State 1

State 1 represents the current system usage. This distribution of stresses has been calculated from the current air wing composition as well as the current system usage. Results from this state are used as a baseline of comparison to the other system states. It can be seen that the distribution of bin usage is relatively uniform. This stems from the mission profile of a non-combat usage profile. When compared to states 3 and 4, the usages of bins 6 and 7 is much lower. This stems from the fact that there is not a need to fly combat equipped aircraft in excess when not in a combat operation.

State 2

This state represents the addition of multiple squadrons of heavy aircraft. Such a shift is already in progress, which is why this state has such a high probability. The shift in this state comes from the greater usage of F-18E/F aircraft, as well as the potential usage of F-35. However, due to complications carrier in development of the F-35, carriers have and will see a greater shift in F-18E/F usage.

State 3

State 3 represents combat operations with the current air wing composition. The lack of a bin 2 usage stems from the lack of flying trainer aircraft. During combat operations there is a need to fly mission capable aircraft, thus the trainers are not flown. The shift of usage in the higher bins comes from the usage of combat specific aircraft. These combat aircraft are both larger, as well as carry heavier payloads. Both of these factors produce a higher usage of bin 6 and 7.

State 4

State 4 is a combination of combat operations and a strong increase in heavy aircraft usage. It can be seen in this state that there is a much greater usage of the more stressful bin when compared to states 1 through 3. This state is based upon the mission profiles of combat operations currently in practice. This known usage pattern was then amplified with the known shifts in air wing compositions. This is possible as changes in the types of combat aircraft, and their respective squadrons, are known. Based on current mission profiles, as well and anticipated shifts in air wing composition, a high possibility for this state has been obtained.

5.4 Simulation Results

The simulation was run for each of the previously mentioned system states and results were collected. The results collected include number of system failures, availability, and mean time to failure. The two primary aspects of the analysis are the number of downing events and the mean time to failure. Table 14 contains a summary of results for the analysis. A quick analysis of this table indicates that stressful states have a negative impact on the performance of the system.

Table 15: Simulation State Results

	System Failures	Availability	Mean time to Failure
State 1	41	93.7	160
State 2	44	93.3	156
State 3	48	92.9	147
State 4	50	92.5	133

System availability was considered to be an invalid form of caparison. This is due to the manner in which it was applied to the study. At the present time there is little information as to the time it takes to repair each component. Because of this a placeholder value was used to allow for the simulation to run. This placeholder value, due to its small time, leads to a higher than actual system availability. Therefore the primary areas of comparison are the number of system failure and the mean time to failure.

System Failures

The impact of system stresses was evident from the results of the simulation. Table 15 shows the percent increase when compared to the current stress profile of the system. It can be seen from these results that an increase in the usage of heavy aircraft has a positive correlation with the number of system failures. These increases are also not of a small magnitude, specifically in state 4. The most extreme case, state 4, shows a very large increase in the number of failures; 21.95%. When taken into consideration, it is evident that the stress profile has a large impact on the reliability of the system.

Table 16: Simulation System Failures

	Number of Failures	Percent increase
State 1	41	NA
State 2	44	7.31%
State 3	48	17.07%
State 4	50	21.95%

An analysis of component failures in each state was done to determine what components played critical roles in system reliability. Figures 21 and 22 are plots of component failures for each state. For each state a plot of failures was created that illustrated the number of failures for the given interval. From the plots of failures, it can be seen that that the NGL, or nose gear launcher, has the most failures. When compared to the improved piston assembly, the difference in number of failures is significant. The bridle tensioner also had a high number of failures across all system states. It can also be seen that the improved piston assembly remains constant in terms of its number of failures. This is because the reliability model for this component is not a stress based reliability model.

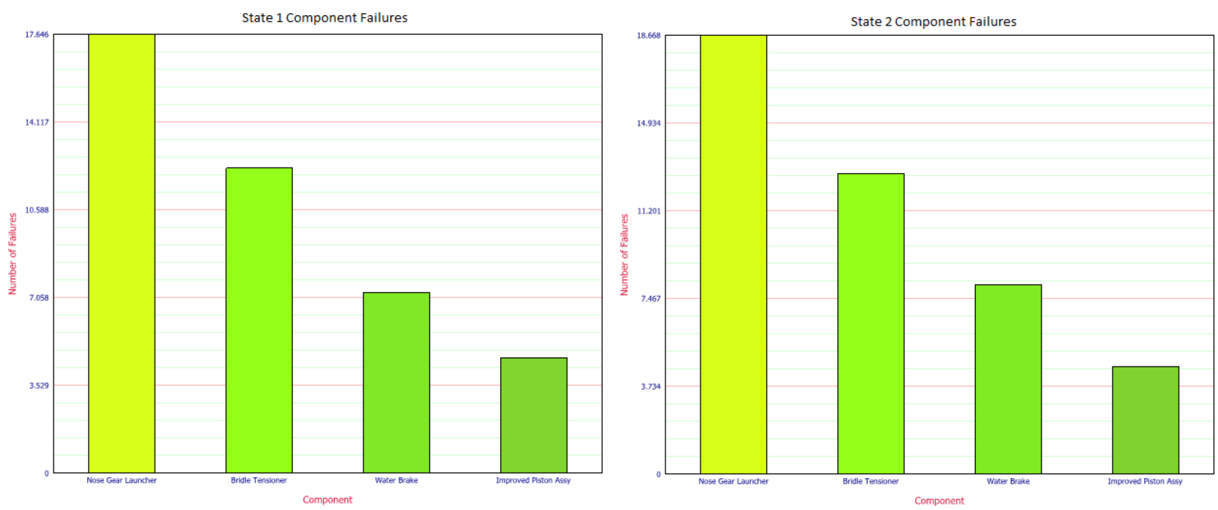

Figure 21: State 1 and 2 Component Failures

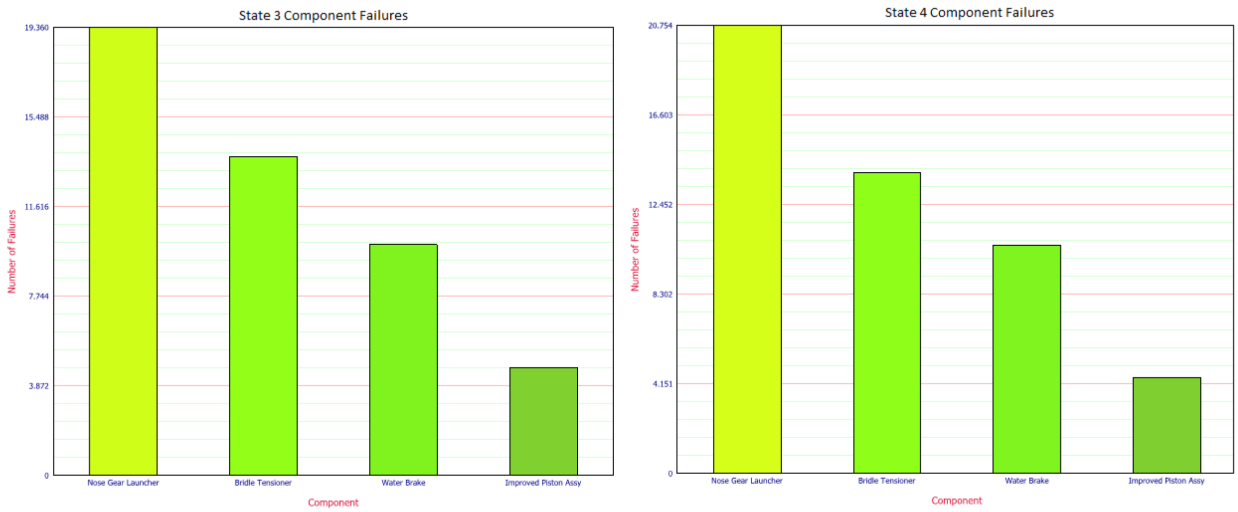

Figure 22: State 3 and 4 Component Failures

The component based analysis of failures shows that the nose gear launcher is the primary cause of system failures. This can be determined because the system is a series system, thus the component with the highest failure rate causes the most system failures. These results indicate that maintenance of the nose gear launcher is critical to the overall operation of the system. It is also apparent that the improved piston assembly is the least critical to quality, as it has the lowest number of failures.

Mean Time to Failure

The second area of interest for the simulation analysis is the mean time to failure of the system. Table 16 shows the decrease in mean time to failure when compared to the baseline state. From the table it can be seen that as the states become more stressful, the mean time to failure decreases. While the magnitude of these values is not as great as that of the system failures, it still shows a negative impact on the system.

Table 17: Simulation State MTTFs

	MTTF	Percent Decrease
State 1	160	NA
State 2	156	2.5%
State 3	147	8.12%
State 4	133	16.87%

From Table 16 it can be seen that State 4 causes a 16.87% decrease in the mean time to failure. This translates to a loss of 33 cycles for the system, or 33 aircraft launches. The combat operations, when combined with the increase in heavy aircraft usage, cause a significant decrease in system reliability. This presents a problem as the possibility for this scenario is extremely likely to occur. It can also be seen that the combat operation state, without the addition of heavy aircraft, has a significant impact on the mean time to failure. This state produces a 8.12% decrease in the mean time to failure.

Weighted Results

The results of the system failures and mean time to failure were weighted according to the probability of the state occurring. This is expressed in Equations 47 and 48. It can be seen that the results for each state are weighted by the probability of the state occurring. The sum is then computed to determine the overall expected number of failures of mean time to failure. This sum gives an estimate of the future state with all possible states taken into consideration.

$$MTTF_{expected} = \sum_{i=1}^{4} P_i \times MTTF_i \tag{47}$$

where i is the state number

$$Failures_{expected} = \sum_{i=1}^{4} P_i \times Failures_i \tag{48}$$

where i is the state number

The results from this weighting process can be seen in Table 17. These predictions represent the weighted predictions in Tables 15 and 16. It can be seen that the value for number of failures shows a 12.2% increase when compared to the baseline. This is not as extreme as the results found for state 4, but is still significant. The weighted value for MTTF shows a slightly lower shift at a difference of 7.5% from the baseline. These results show that when all future states are taken into account there exists a less reliable trend. This finding is important as it indicates that all possible states have a noticeable weighted impact in system reliability.

Table 18: Weighted Results

	Weighted Value
Number of Failures	46
MTTF	148

5.3 Analysis of Results

Results from these simulations provide insight as to how changes in air wing compositions and usage impact the performance of the catapult system. It can be seen that increases in composition alone have only a slight effect on system mean time to failure and the number of system failures. Combat operations, without a change in air wing, produce a larger impact on reliability than changes in air wing composition alone. This result indicates that the usage pattern is critical to system reliability. The simulation in which there were changes in air wing composition and combat operations produced a significant impact on the system reliability. This scenario yielded a 21.95% increase in system failures and a 16.87% decrease in mean time to failure. Such changes are not negligible and preparation for such a scenario is extremely important. The component specific analysis of failures indicated that the nose gear launcher was the critical component to system operation. This component had a much larger number of failures when compared to the other catapult components.

6.0 Analyses of Maintenance Polices

While the analysis of corrective maintenance polices is not valid, it is still possible to assess the current preventative maintenance policies. Currently, there exist maintenance practices that take place at set intervals. These practices are intended to detect unacceptable component conditions and prevent unexpected component failures. The goal of this analysis is to determine if the current maintenance intervals are acceptable when the future stress states are applied. The states used are the states mentioned in Section 5. Key results in this analysis are the number of system failures and component failures. These metrics are used because it is important to determine it the preventive maintenance can be applied before a component, or system, failure. NAVAIR is concerned that the decrease in MTTF, with the more stressful future states, will lead to an increase in failures before they can be detected.

Results are generated using a simulation in Blocksim. The approach to this simulation is similar to that of Section 5. The key difference is the addition of preventive maintenance actions. These actions, in theory, should affect the number of failures that occur. Results and finding are compiled in a similar manner. A total of 500 simulations were run, each at an interval of 10,000 cycles. The system states applied to the components can be seen in Table 18.

Table 19: System State Values

	Bin 1	Bin 2	Bin 3	Bin 4	Bin 5	Bin 6	Bin 7
State 1	.05	0.15	0.1	0.25	0.10	0.2	0.2
State 2	0.05	0.1	0.1	0.15	0.10	0.3	0.2
State 3	0.1	0	0.05	0.1	0.15	0.30	0.25
State 4	0.05	0	0.05	0.1	0.15	0.35	0.30

The current maintenance polices can be seen in Table 19. The time the maintenance is preformed is in cycles, or aircraft launches. These polices are based on the current mission profiles and air wing compositions. The actions listed take into considerations the wear rates based on these current stress profiles. The maintenance actions for each component are used as inputs into the simulation model. Each component in the model will have its respective preventive maintenance action within its block. The maintenance policies remain the same through all the system states.

Table 20: Maintenance Policies

Component	Maintenance Interval (cyc)
NGL	450
Bridle Tensioner	750
IPA	1000
Water Brake	1000

Results from the simulation can be seen in Table 20. This table contains the total number of failures for the system, as well as the number of times each component failed. System failures in the simulation are caused by insufficient preventative maintenance. By this it is meant that if a preventive maintenance interval is greater than the time to failure, a component or system failure is recorded.

Table 21: Maintenance Simulation Failures

	Total Failures	NGL	BT	IPA	WB
State 1	51	23	14	7	7
State 2	53	24	15	7	7
State 3	56	25	15	7	9
State 4	59	26	16	7	10

From the results it can be seen that at the states become more stressful, the relative number of failures increases. In the most stressful case, state 4, there is an increase of 15.6% in the total number of failures. The IPA appears to be unaffected by changes in stress state. This is potentially due to the maintenance interval being short with respect to the changing MTTF. The bridle tensioner also only has a slight increase in the number of component failures. Figure 23 shows a comparison of all the components for each state. This graph shows a side-by-side comparison of each component with respect to the number of failures.

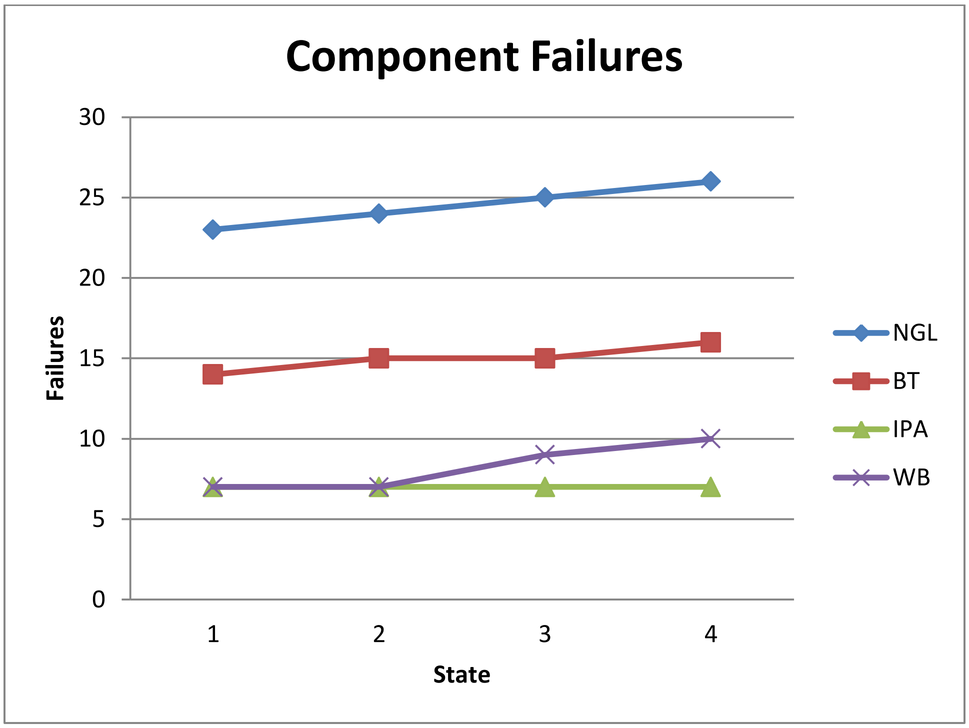

Figure 23: Component Failures by State

Maintenance results

Results from this analysis indicate what components require improved maintenance policies. Because the improved piston assembly shows no increase in the number of failures, it can be determined that there is no need to improve the maintenance policy for this component. The nose gear launcher was found to have a significant increase in the number of failures. This implies that the current preventative maintenance policies are not capable of handling the increase in failures. In a similar manner, the water brake showed a significant increase in the number of component failures. This component had a 42.7% increase in the number of failures. The bridle tensioner only had a modest increase in the number of failures that occurred, and the impact is questionable.

From these results it is apparent that the water brake and nose gear launcher require an improvement to their maintenance polices. These revised policies require the knowledge and expertise of NAVAIR, and cannot be arbitrary. This study showed the critical components in terms of failures, but with the current information it is difficult to create revised maintenance policies. Such action requires information about maintenance crew availability and the acceptable number of failures for the system or component. Once the required information is obtained, it becomes possible to simulate multiple possible maintenance policies to determine the optimal policy.

References

Ajodhya, N. D. & Damodar, A. "Age Replacement of Components During IFR Delay Time." *IEEE Transactions on Reliability*, 2004: 306-312.

Hada, A., Coit, D., Angello, M., & Megow, K. "System Reliability Models With Stress Covariates for Changing Load Profiles." *RAMS Symposium*, 2011.

Jonhson, D., Kosaka, R., Coit, D., Agnello, M., & Megow, K. "Constrained Maximum Likelihood Optimization." *RAMS Symposium*, 2013.

Laura, A., Maurizio, G., & Gianpaolo, P. "A Mixed-Weibull Regression Model for the Analysis of Automotive Warranty Data." *Reliabiltity Engineering and System Saftey*, 2008: 265-273.

Mettas, A. "Reliability Predictions based on Customer Usage Stress Profiles." *Reliability and Maintainability Symposium.* Alexandria: IEEE, 2005.

Prasad, P.V.N., & Rao, K.R.M. "Reliability Models of Repairable Systems Considering the Effect of Operating Conditions." *Relaibility and Maintainability Symposium.* Osmania: IEEE, 2002. 503-210.

Sylvain, L., Fazel, F., & Stan, M. "Data Mining For Prediction of Aircraft Component Replacement." *Intellegent Systems and their Applications*, 1999: 59-66.

Wang, Z., Xie, L., & LI, B. "Reliability Model of Failure-Dependent System with Frequency of Loading Taken into Account." *Journal of Northeastern Univeristy(Natural Science)*, 2007: 704-704.

Xiang, Z., & Ernst, G. "Component Reliability Modeling of Distribution Systems Based on the Evaluation of Failure Statistics." *IIE Transactions on Dielectrics and Electrical Insulation*, 2007: 1183-1191.

Zheng, W., & Rui, K. "Failure Rate Model of Components with the Number of Load Applications as a Life Parameter." *Reliability, Maintenance and Saftey*. IEEE, 2009. 241-244.